UNIVERSITY *of* WASHINGTON

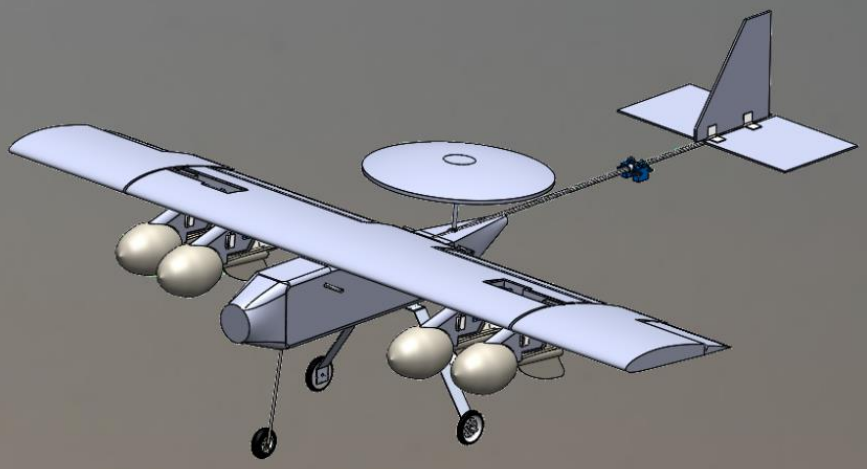

AIAA Design, Build, Fly

2018-2019

Table of Contents

Abbreviations, Acronyms, Symbols, and Variables

Acronym	Description
AIAA	American Institute of Aeronautics and Astronautics
AOA	Angle of Attack
CAD	Computer Aided Design
CFD	Computational Fluid Dynamics
DBF	Design Build Fly
FEM	Finite Element Method
NACA	National Advisory Committee for Aeronautics
PLA	Polylactic Acid
RC	Remote Control
RFP	Request for Proposal
RPM	Revolutions per Minute
UW	University of Washington
AR	Aspect Ratio
b	Wingspan [m]
c	Chord [m]
Cd	Coefficient of Drag
CG	Center of Gravity [m]
Cl	Coefficient of Lift
d	Diameter [m]
D	Drag [N]
F	Force [N]
g	9.81 m/s^2
L	Lift [N]
P	Power [W]
Pr	Power Required [W]
S	Surface Area [m^2]
Slo	Rolling Takeoff Distance [m]
T	Thrust [N]
t	Time [s]
Tr	Thrust Required [W]
Vh	Horizontal Tail Coefficient
Vv	Vertical Tail Coefficient
w	Weight [N]
rho	Density [kg/m^3]

1. Executive Summary

1.1 Solution Design Summary

For the academic year 2018-2019, the Design Build Fly team at the University of Washington designed, built, and tested a remote-controlled aircraft named Squawk 7700. This aircraft must be capable of supporting aircraft carrier operations. It must also have folding surfaces that allow for a stowed configuration. Physically, the aircraft must have a minimum wingspan of four feet, and be able to take off from a 4x10 ft. ramp angled at five degrees from horizontal. In its stowed state, the aircraft must also be able to roll through a 3x2 ft. box without interference. The nose and landing gear must fit within the box depth of 2 ft. Finally, the aircraft must be able to transition from folded to flight configuration remotely, as well as mechanically locking itself. At the time of competition, the plane must also complete the three flight missions and a single ground mission.

First, the aircraft must complete a flight with no payload onboard. Following that, the aircraft must be able to fly the course with the radome attached to successfully complete the Reconnaissance mission. The third mission involves the attack stores, where a minimum of four must be mounted onto the plane, with one dropped independently on the downwind leg of each flight. Lastly, members of the ground crew must be able to quickly equip and detach the stores and radome elements from the aircraft during the ground mission.

1.2 Design Solution Summary

After analyzing all mission and physical requirements, it was determined that drag resulting from the stores and radome would be the most significant challenge this year. The other significant challenge was to achieve enough lift rapidly in order to takeoff in such a short distance. Therefore, it was decided that maximizing lift and reducing empty weight were the most critical components for the design. A monoplane configuration that utilizes an extended chord wing and large flaps was identified as the best solution to maximize lift while keeping system complexity to a minimum. The aircraft must be capable of flying around 20 mph to meet the five minute time window for each mission, therefore, weight minimization was emphasized as a critical design requirement. The aircraft body was constructed primarily from polystyrene due to its light weight and excellent durability, with a carbon fiber spar running through the wing to maintain rigidity, and a carbon fiber longeron running through the fuselage. At the rear of the aircraft, the horizontal and vertical stabilizers mount directly to the carbon fiber spar in a conventional tail arrangement.

Mechanisms for a wing folding design, radome, and dropping the attack stores posed unique challenges. These components had to be able to perform their required functions while adding minimal

weight and drag to the design. It was determined that the drop mechanism, wing folding mechanism, and radome would be constructed almost entirely out of polystyrene or 3D printer filament in order to minimize their weight and allow for replacement components to be easily and cheaply created. In addition, it needed to be ensured that the radome and attack stores were easily attachable and removable. Therefore, simplifying their design as much as possible became a necessity.

The monoplane configuration proved to be ideal for fold-down mechanisms that were effective at reducing the wingspan of the plane for its stowed configuration. A hinging and mechanically locking mechanism was designed that allowed for the wings to fold directly downward on both sides, which allowed the plane to be reduced to the required sizing for stowing. This mechanism was designed to be 3D-printed, and entirely contained within the wing in order to have minimal impact on aircraft drag.

2. Management Summary

2.1 Team Structure

The 2018-2019 UW DBF team consists of approximately 30 students who participate as an extracurricular activity. The roster consists of 2 seniors, 5 juniors, and 23 sophomores or freshmen. The team is filed under the UW as a student-led club, augmented by guidance from the faculty advisor, Dr. Chris Lum. Furthermore, individuals who are employed in the aviation industry offered suggestions. The leadership structure of UW DBF is outlined in the management chart in Figure 1. All members of the leadership team take on a specific administrative role alongside their primary engineering role.

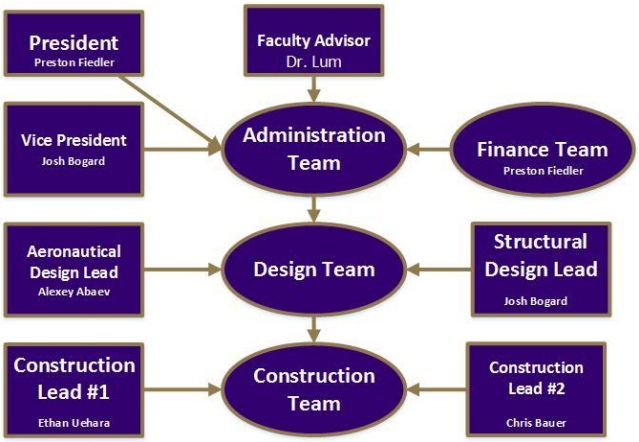

Figure 1: Management Chart

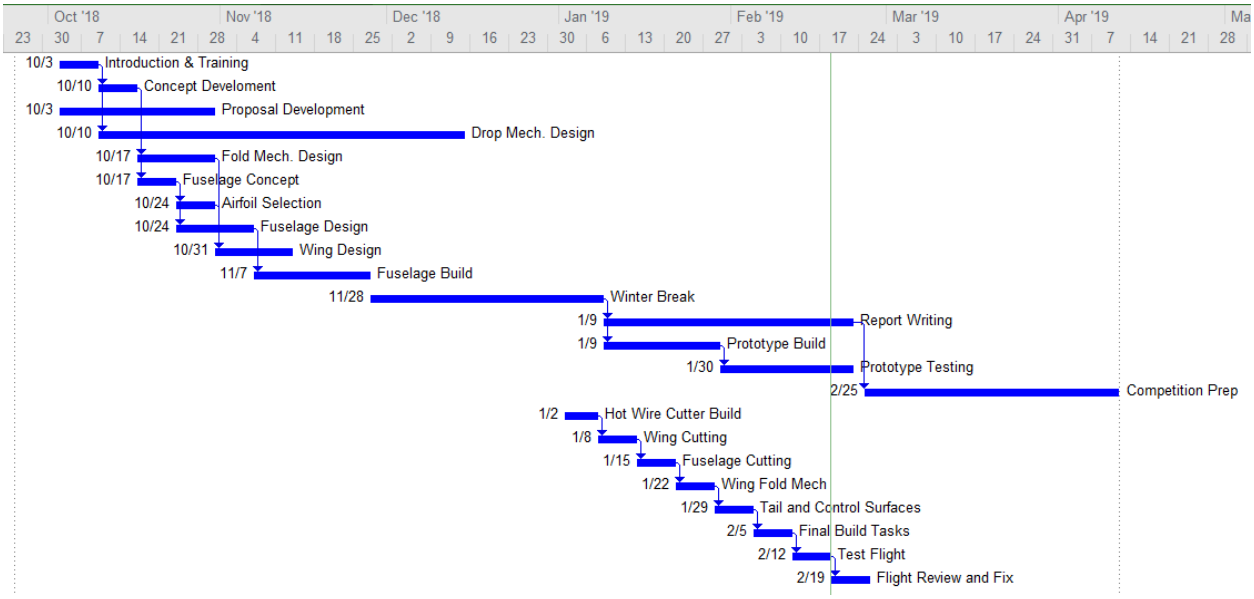

Figure 2: Program Schedule

Figure 2 outlines the methods of tracking project progress. Major milestones are marked by vertical lines, and the fly-off dates are marked by the dashed line. The design process began with a detailed analysis of the RFP and an examination of competition scoring. Initial design research maximized the score, while keeping production complexity and cost as low as possible. Once a preliminary design concept was selected, work began on sizing, airfoil selection, and motor selection. During the initial design phase, design refinement through simulation, as well as rapid prototyping were the primary areas of focus to identify and resolve any major issues before flight. Upon selection of the motor, propeller, airfoil, and general design, the aircraft was constructed. After additional testing and submission of this report, the aircraft will be optimized for competition by reducing weight and improving component quality.

3. Conceptual Design

3.1 Mission Requirements

There are three flight missions and one ground mission that must be completed at competition. The following flight missions must be completed on the course depicted in Figure 3.

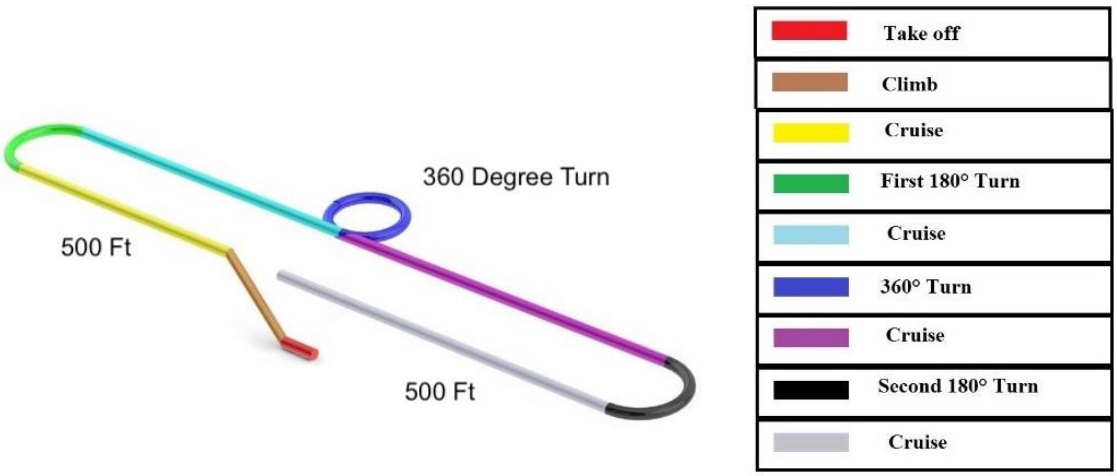

Figure 3: Competition Flight Path

3.1.1 Delivery Mission

For the first flight mission, the aircraft has no payload. The aircraft must be remotely commanded from the stowed configuration to flight configuration, including a wingtip locking feature check, within a 5 minute staging period. Before takeoff, a crew member will restrain the aircraft by the tail hook while being powered up, and it will be release upon pilot command. Takeoff will then take place from the ramp which is 10 feet long at an angle of 5 degrees to the horizontal. From the time when the aircraft is released, there is a 5 minute flight window in which 3 laps must be completed. After 3 laps are completed, the aircraft must complete a successful landing on the runway in order to register a score. Scoring for this mission is solely based on successful completion of the 3 laps.

3.1.2 Reconnaissance Mission

For the second flight mission, the aircraft has a rotating radome as its payload. The radome must be installed on the aircraft in the staging box within the 5 minute staging period. Once the aircraft has taken off and completed the first 180 degree turn, the radome must start rotating and continue to rotate until the final 180 degree turn. After 3 laps are completed during the 5 minute window, the aircraft must complete a successful landing in order to register a score. Scoring for this mission is dependent on mission time relative to other teams, with higher scores corresponding to faster times.

3.1.3 Attack Mission

For the third flight mission, the aircraft has attack stores as the payload. The number of attack stores validated during the tech inspection must be installed in the staging box during the 5 minute staging period. Once the aircraft tail hook is released by the flight line crew member, the 10 minute window for this mission starts. Teams must then complete as many scoring laps as possible in this 10 minute window. A scoring lap is a completed lap in which the aircraft successfully releases an attack store on the

downwind leg of the pattern. Upon completion, the aircraft must complete a successful landing in order to register a score. Scoring for this mission is dependent on the number of scoring laps completed, with higher scores corresponding to more completed scoring laps.

3.1.4 Ground Mission

The aircraft must undergo a timed ground demonstration of missions 3.1.2 and 3.1.3. The aircraft will begin in its stowed configuration inside the 10 foot by 10 foot mission box, along with the 4 attack stores and uninstalled radome. Only assembly crew members are able to touch the aircraft during the ground demonstration. The aircraft must remotely transition into its flight configuration, and then assembly crew members must install the radome. Time will then pause, and the pilot will demonstrate ability to remotely activate the rotating radome. Next, assembly crew members will return to the mission box to remove the radome and install 4 attack stores. Time will then stop and the pilot will demonstrate that propulsion and controls systems are working, as well as that the attack stores are able to be released individually to complete the mission.

3.2 Design Requirements

After closely analyzing the requirements of the 3 flight missions and the ground mission, key design requirements for mission success were identified.

Before addressing the key design requirements imposed by the mission requirements, it was identified that the competition location could pose some unique weather-related challenges. Since the flight testing occurs at the University of Washington, which has considerable climate differences with the Tucson fly-off sight, the design of the aircraft took weather disparities between the locations into account. Trade studies were performed researching climate trends in Tucson in April. It was determined that humidity and precipitation would be a non-factor, as the average monthly rainfall is less than an inch. However, this is a sharp contrast to much cooler and more humid Seattle where the aircraft is designed and tested, so certainty that the aircraft would not have its performance altered in differing weather conditions was key.

Perhaps the largest potential impact that weather has on the competition comes from wind. The average mean hourly wind speed in April in Tucson is 8.7 mph, with a 10th percentile of 3.6 mph and a 90th percentile of 16.1 mph. This data has a large impact on aircraft performance, so the aircraft needed to be designed to operate well in these conditions. Additional points of concern were the temperature and altitude. The average high temperature over the competition days is 82 degrees Fahrenheit, and the average low temperature over these days is 53 degrees Fahrenheit. The altitude of the testing location is 2,643 feet, which is an important factor when accounting for air density and pressure for flight conditions.

Beginning analysis of the mission requirements, the first challenge identified was the requirement of taking off from a 10 foot ramp at a 5 degree angle. Especially with the additional weight and drag that would inevitably be added to the aircraft with the addition of attack stores and a radome, achieving a high enough takeoff speed within 10 feet was identified as a major design concern. Thus, it was a primary design requirement for all of the flight missions that the aircraft would be able to generate enough power and lift in order to takeoff on the shortened runway.

The next challenge identified was being able to remotely transition the aircraft from stowed configuration to flight configuration. The aircraft wingspan must be a minimum of 4 ft., and the aircraft must be able to roll through a 3 foot by 2 ft. space. In order to accomplish this, it was necessary to design a mechanism that would allow the wings to fold down or reposition remotely such that the wingspan is reduced by a minimum of one foot.

The last major design challenge identified was the ability to individually drop a minimum of 4 attack stores while in flight. Per the requirements, no part of the plane is allowed to be dropped with the attack stores. In addition, the pilot must have control over the timing of drops in order to ensure that they occur on the downwind leg of each lap. It was crucial to design an attack store dropping mechanism that would allow for individual dropping while adding minimum weight and drag to the aircraft, as any unnecessary weight or drag would only increase the difficulty of taking off within the length of the ramp. Of equal importance was ensuring that the aircraft maintain stability and control authority while in an asymmetrical loadout.

3.3 Solution Concepts/Configurations Considered

For each of these design challenges, numerous solutions were considered before research and testing was conducted in order to determine the ideal configuration.

3.3.1 Aircraft Sizing

In order to takeoff within the 10 foot long runway, it was obvious that a balance would have to be achieved between aircraft weight, lift, and acceleration. The main consideration here was whether to design a larger aircraft with the largest wingspan possible and a powerful motor, or a smaller aircraft that would accelerate faster and have a lower takeoff velocity. Ultimately, the payload requirements for the provided missions made it clear that a larger aircraft with near maximum wingspan would be advantageous for numerous reasons. The aircraft must be able to support at least four attack stores on the wings, so a large, more massive fuselage would be in order to better resist the moment of the wings. Mounting the necessary servos and control rods was also much easier on a large fuselage. Furthermore, larger wings would provide more lift to overcome the additional weight of the attack stores. Also, for the reconnaissance mission the radome had to be a minimum size. It was determined that the negative aerodynamic impact produced by the radome would be proportionally less on a larger aircraft than a

smaller aircraft. Therefore, it was decided that it was advantageous to focus on a large fuselage and wingspan, supported by a more powerful motor.

3.3.2 Stowed Configuration Mechanism

Due to the restrictions placed on aircraft sizing in stowed configuration, a mechanism was required that would allow the wingspan to be remotely reduced when on the ground. After brainstorming, it was determined that this could be accomplished either by sweeping the wings back, by sliding the wing such that both sides could slide inward and overlap over the fuselage, or folding the wing tips down on both sides.

The first design proposal, the wing sweep had a servo mounted in the fuselage. This servo would have been modified for continuous rotation, enabling it to wind strings or rubber bands around its servo horn. These strings or bands would have been connected to the leading edge of the wing roots. The winding of the strings and bands would therefore pull the leading edges of the wing in and forward, un-sweeping the wings. Due to its early consideration and ultimate rejection, the possibility of needing a similar mechanism to sweep the wings was not addressed. A main issue with this setup was the moment of airflow on the wing extensions that had to be resisted, in order to keep the wingtips aligned.

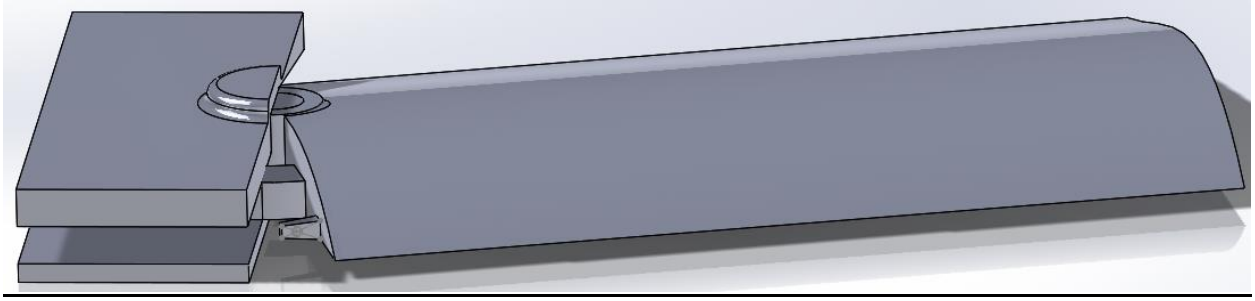

Figure 4: Wing Sweep Design

The second proposal, the wing slide mechanism, had wing extensions sliding out from on top of the main wing section. This design would have had a micro servo driving an PLA plastic 3D-printed linear actuator to pull the wing sections in and push them out. To keep the wing extensions inline with reference to the lateral axes, the wing extensions slid through two guides mounted to the top of the main wing, on both sides. This design would have ultimately had the wing extensions raised higher than the rest of the wing. While the sliding design needed to resist less moment on its extensions, its main drawback came from the drag generated by the parts placed on top of the wing.

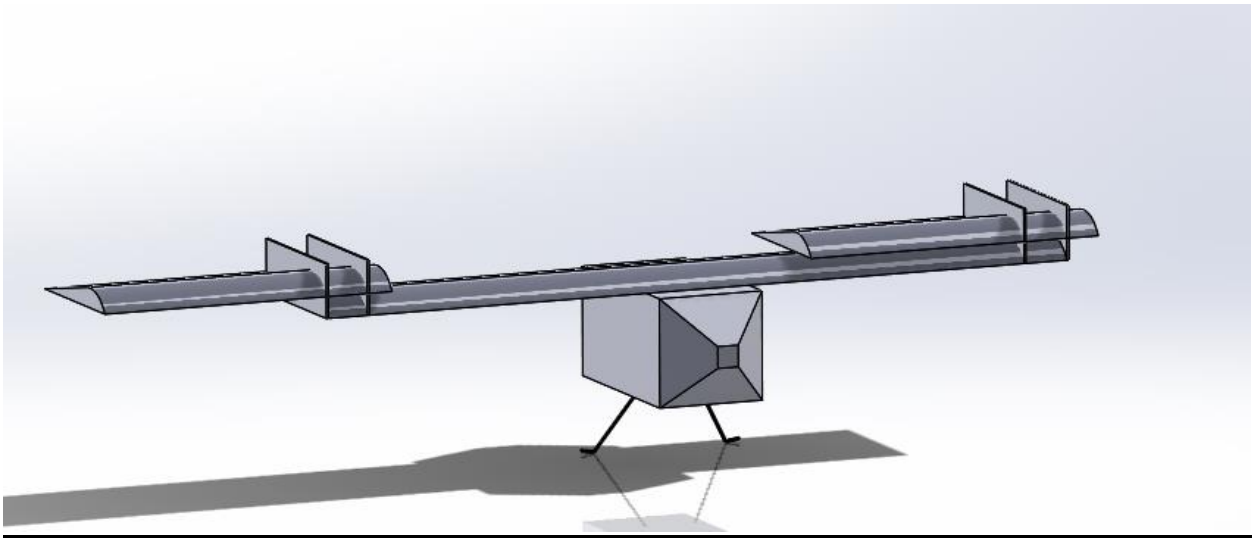

Figure 5: Wing Slide Design

The final proposal was a wing folding mechanism. The initial design for this proposal involved the possibility of using a servo-driven linear actuator on the underside of the main wing to slide out a pin to push the wing fold up, inline with the rest of the wing. The second design, inspired by the wing folding mechanism of a RC Corsair, used a servo to rate a threaded shaft to pull in a screw that was attached inner side of the of the wing fold. This mechanism was embedded in the wing itself and pulled the wing fold flush with the rest of the wing. Removing the mechanism from the air flow made it the most aerodynamic of the options. Due to the main force exerted on the wing extensions acts opposite the upwards lift, the moment keeps the wingtips in the desired, folded up and extended position.

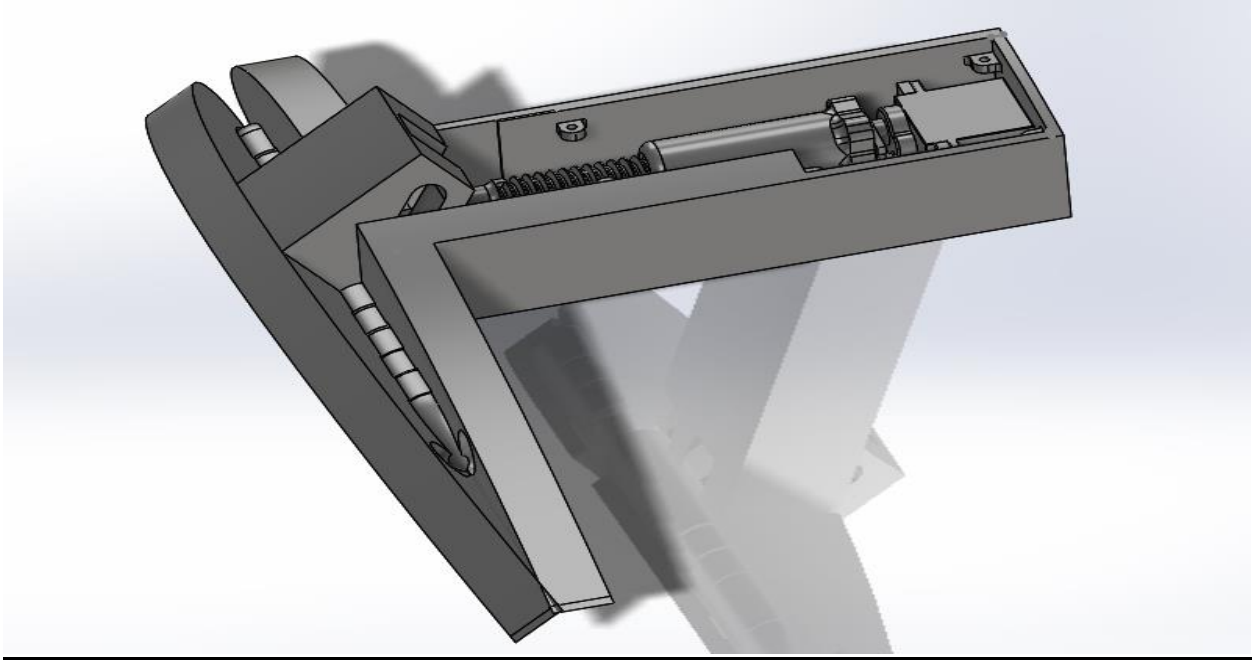

Figure 6: Wing Fold Mechanism Design

The table below summarizes the decision process, with the advantageous proposal highlighted in green for each consideration.

Consideration	Wing Sweeping	Wing Sliding	Wing Folding
Wing Alignment	Yes	No*	Yes
Relative Weight (total)	25 grams	100 grams	100 grams
Size (by Volume)	Similar to Wing Slide and Fold	Similar to Wing Sweep and Fold	Similar to Wing Sweep and Slide
Mechanism Location and Effect	Fuselage	On Top of Wings	Inside Wings
	Uses Electronics Space	Airflow Disruption	Reduced Drag

Forces Moments Sustained by Mechanism	Drag produced by Wing	Lift and Drag produced by Wing Extension	Moment of Wing Fold's weight during fold movement
Locking Mechanism Simplicity	Similar to Wing Slide and Fold	Similar to Wing Sweep and Fold	Similar to Wing Sweep and Slide
Relative Overall Complexity	Simplistic	Highly Complex	Complex

**wing slide alignment would have added significant complexity*

Table 1: Concept Scoring

Ultimately the wing folding proposal was chosen for its ability to keep the wing sections in alignment by having the mechanism inside the wing and out of the airflow. The lack of forces and moments acting on the mechanism during flight, its positioning in the wings, and its low complexity give it an advantage over the more complex sliding design.

3.3.3 Attack Store Drop Mechanism

Per attack mission requirements, four attack stores had to be able to be mounted onto the aircraft. These stores must be remotely dropped on command, and no part of the aircraft is allowed to drop along with the stores. Numerous mechanisms were designed in SolidWorks and analyzed in order to determine the optimal solution.

The first mechanism resembled a modern gate latch, where a spring-loaded latch could lock an attack store into place between two metal plates. The spring loading mechanism would be very easy to quickly load, and it would provide enough force to ensure that the stores would not accidentally release before they were intended to do so. However, there were too many negatives associated with this design for it to be used. The metal plates facing perpendicular to the length of the airplane had a large surface area which would generate unnecessary drag, and the spring loading would require a large force to initiate the release of the stores. There is also a high chance that the attack stores would not fall immediately when the latch was removed, resulting in inconsistency with drop accuracy.

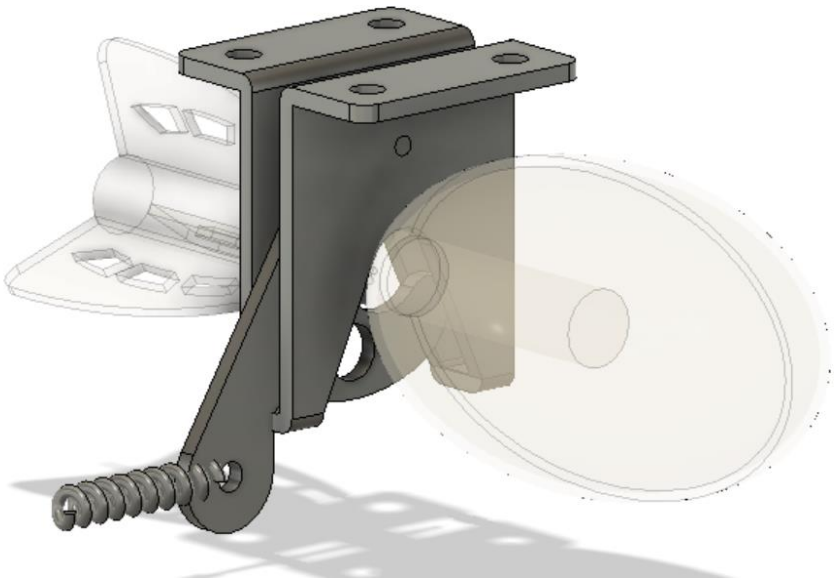

Figure 7: Gate Latch Drop Mechanism

The next mechanism that was considered consisted of two arms that would go down around both sides of the stores, forming a circle around them. A control rod would be pulled from the top, opening the arms and allowing the stores to fall. This design was very enticing because of the very small cross-sectional area and weight, but ultimately the complexity of this design made it impractical for construction and implementation.

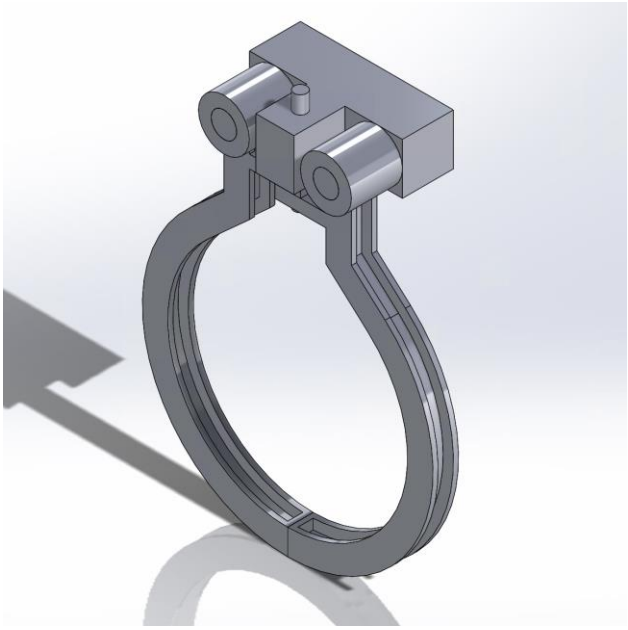

Figure 8: Moving Arms Drop Mechanism

Another design consisting of vertical pylons with stores secured to the ends by rubber bands was also considered. Rubber bands would be secured on one side of the pylons, loop around the store at the end, and then connect to a servo controlled pin on the other side of the pylon. When activated, the servo could pull the pin which allowed the store to fall freely from the pylon. This design was advantageous because it could be loaded very quickly and the vertical pylons would offer significant resistance to pitching forces. Additionally, the simplicity of the mechanism would make the dropping process simple and repeatable. However, analysis of this mechanism quickly determined that it offered too little resistance to horizontal swaying of the stores. While inflight, the stores would be free to vibrate and pivot from side to side, which would impose significant challenges when trying to control the aircraft. The vertical pylon itself was also much larger than it needed to be in this design, and would have contributed excessive amounts of drag to the aircraft.

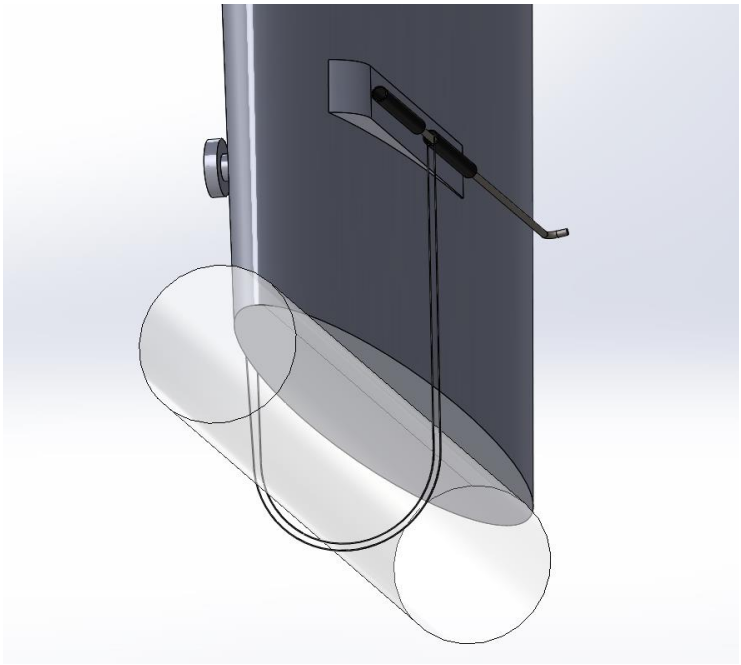

Figure 9: Rubber band pylon drop mechanism

With one of the primary design limitations being the number of servo motors that could be supported by remote controller, multiple designs were considered that attempted to control the release of multiple stores via a single servo motor. The most polished of these designs involved a gearing mechanism, where a servo actuated dual pin could slide in both directions, individually releasing two stores with a single servo motor. This mechanism was desirable because it would enable one servo motor to control the release of both stores on each side of the wing, allowing just two servo motors to control the release of all four attack stores. Ultimately, it was the complexity of integrating this idea that pushed this design out of consideration. Other considered mechanisms were much simpler and proved to be much more reliable for accurately dropping the attack stores.

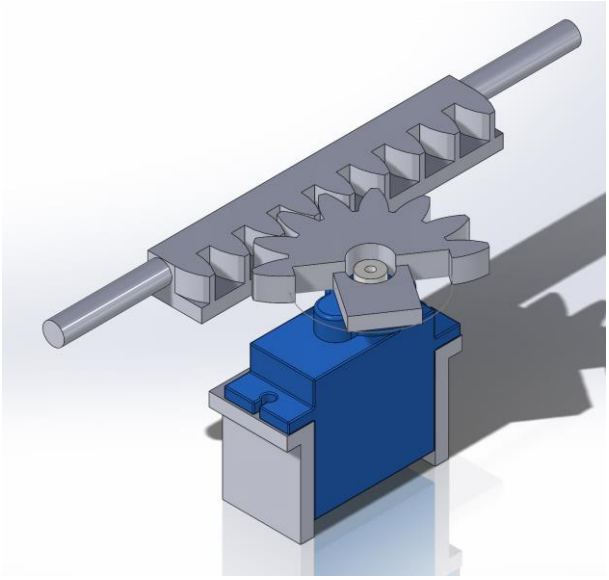

Figure 10: Servo-actuated dual-pin drop mechanism

The advantages and disadvantages of each drop mechanism design were listed out in Table 2 and comparisons were made to determine the most versatile drop mechanism. The rubber band design was ultimately selected (Table 3).

Concept	Advantages	Disadvantages
Gate Latch	• Quick to load	• Large forward surface area • Large actuation force • Large release travel • Complex servo integration
Moving Arms	• Lightweight • Small forward surface area • Low release force with pin	• Complex shape • Lacks torque support • Large release travel • High part count (>7) • Slow to load • Complex servo integration

Rubber Band	• Small forward surface area • Pitch and torque support • Low release force • Low release travel • Simple servo integration	• Large overall surface area
Servo Dual Pin	• Control two stores with servo	• Complex mechanism • Complex mechanical release • Slow loading time

Table 2: Pros and Cons of Drop Mechanism Designs.

Concept	Gate Latch	Moving Arms	Rubber Band (Selected)	Servo Dual Pin*
Load Speed	Fast	Slow	Fast	Slow
Fwd Sfc Area	Large	Small	Small	Small
Actuation Force	High	Low	Low	Low
Release Travel	High	Low	Low	Low
Servo Integration	Complex	Complex	Simple	Complex
Torque Support	High	Low	High	High

Table 3: Factor Comparison of Drop Mechanism Concepts

4. Preliminary Design

4.1 Design Methodology

In creating the preliminary design for the aircraft, the first step was to estimate the total weight of the aircraft. This weight estimate was then used to perform early aerodynamic calculations determining the required lift and thrust of the aircraft, as well as the resulting drag. These performance requirements were then used to come up with initial sizing estimates for all aspects of the aircraft. Using these rough estimates, a rudimentary model would be constructed in RealFlight 8 in order to test the airfoil, control surfaces, and power system to determine if the initial calculations were accurate and feasible. After testing in RealFlight, a detailed SolidWorks model of the aircraft was created and the flow simulation plugin was used to determine more realistic lift and drag properties.

Once initial aerodynamic designs were engineered, the design was analyzed to determine what would be structurally required of the system. During this step, materials and methodologies for construction were reviewed to determine if the design could structurally resist the loads being placed upon it.

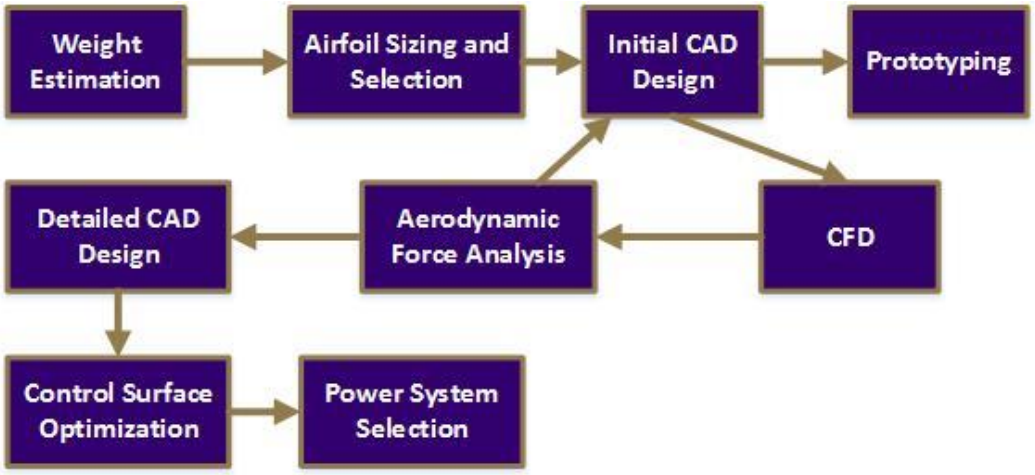

Figure 11: Design Methodology Flow

4.2 Design Sizing

4.2.1 Weight Estimates

Before beginning the design process, rough weight estimates had to be made for the aircraft. This was accomplished using a combination of aircraft geometry, material properties, component weights, and

data from previous competitions. These calculations were done conservatively in order to leave room for manufacturing processes not being able to produce ideal parts. The empty weight of the aircraft was initially calculated to be a maximum of 4.5 lbs, and the weight of the aircraft with its maximum payload was conservatively calculated to be 6 lbs. These weights were the primary factors considered when beginning to select and design the rest of the aircraft.

4.2.2 Airfoil Selection and Wing Sizing

The first part of the design process was determining a suitable airfoil and wing size for the aircraft. Due to manufacturing restrictions, it was decided to not consider heavily cambered airfoils. Data and graphs from the NACA airfoil database were thoroughly analyzed. These graphs were initially compared visually to corresponding graphs of similar airfoils in order to narrow down options, and then MATLAB simulations were performed to predict resulting lift and drag on the aircraft for each analyzed airfoil. After numerical analysis of a wide range of airfoils in MATLAB, it was decided that the NACA 4412 airfoil was optimal for design needs due to its high lift coefficient and Cl/Cd ratio within the desired operable angles of attack.

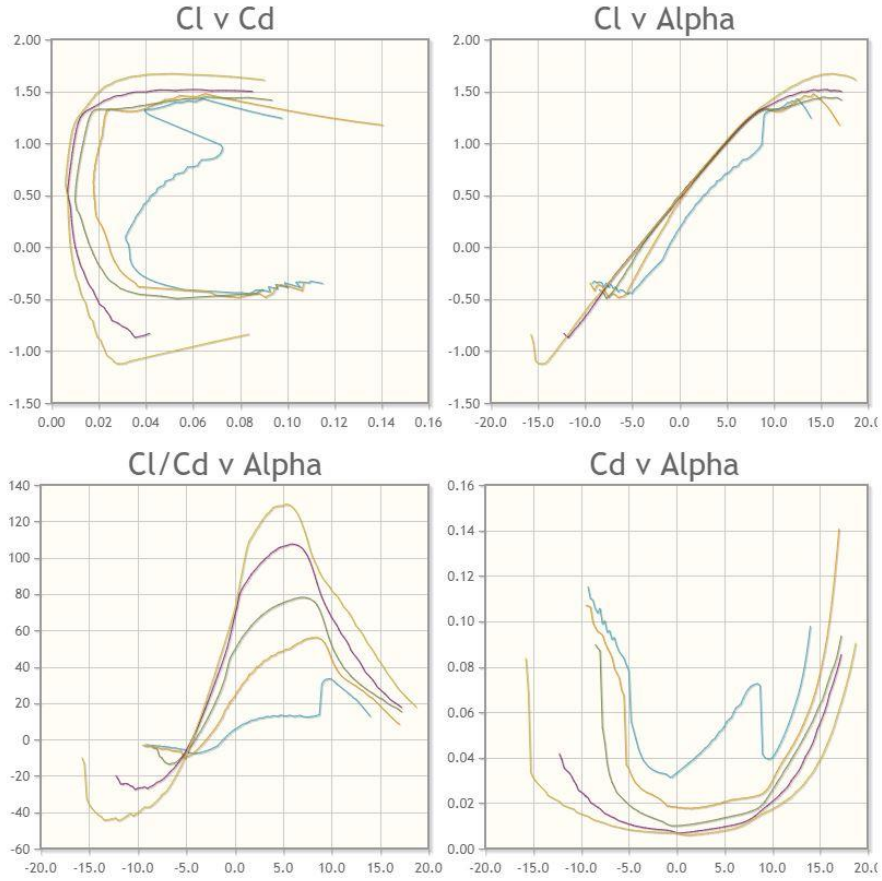

Figure 12: Coefficients of Lift and Drag Graphs (NACA 4412)

The mission requirements state that the wing must have a minimum span of 4 feet and be able to reduce to a 3 foot wingspan when in stowed configuration. Due to the short required takeoff length, it was deemed optimal to maximize the aircraft's span within these sizing requirements. Ultimately the wing was designed in three parts; a center section above the fuselage and two smaller sections on both wing tips. The center section was maximized such that it could still roll through the 3x2 foot box, so it was designed to be 34 inches wide to leave room for the wing folding mechanism protrusion and a small space buffer. Utilizing the folding mechanism, both sides of the wing had 9 inches of folding wing that could be raised, lowered, and locked remotely when transitioning between stowed and flight configuration. The 9 inch size was chosen because it was the maximum amount of wing that could be folded down without risking striking the ground, and because of load limitations on the servo motors. In flight configuration, the aircraft was designed to have a wing span of 52 inches.

When determining the wing chord and thickness, the two primary considerations were required lift and the ability to mount the store dropping mechanisms underneath the wing. Aerodynamic analysis was performed on the wing to determine the chord sizing necessary to generate the required lift. The optimal chord size was determined to be 9.5 inches, so the chord was initially conservatively designed to be 10 inches. This results in a thickness of approximately 1.5 inches, which is also thick enough to mount the store drop mechanism. Thus, the preliminary dimensions of the aircraft are detailed in Table 4.

Span (in)	Chord (in)	Thickness (in)	Surface Area (in^2)	Aspect Ratio
52	10	1.5	494	5.47

Table 4: Preliminary Aircraft Sizing

4.2.3 Tail Sizing:

Equations 1 and 2 were used to determine approximate dimensions for the tail size. Given the dimensions of the aircraft, the horizontal and vertical tail volume coefficients were calculated. A well-behaved aircraft typically has a horizontal tail volume coefficient of between 0.30 and 0.60, and a vertical tail volume coefficient of between 0.02 and 0.05. Initially, the horizontal stabilizer was designed to have a surface area of 108 square inches, and the vertical stabilizer was designed to have a surface area of 53 square inches. Based on the measured wing size and moment arm, these values yielded a horizontal tail volume coefficient of 0.43 and a vertical tail volume coefficient of 0.024. These tail volume coefficients fall within the range of standard values for well-behaved aircraft.

$$V_h = \frac{S_h l_h}{Sc} = 0.43$$

Equation 1: Horizontal tail volume coefficient

$$V_v = \frac{S_v l_v}{Sb} = 0.024$$

Equation 2: Vertical tail volume coefficient

After determining the size of the tail, the size of the elevator and rudder needed to be calculated. Typically, well-controlled aircraft have elevators and rudders approximately ¼ to ⅓ the surface area of the vertical stabilizer and horizontal stabilizer respectively. Due to the control requirements of the aircraft, it was determined that rudder and elevator sizing should fall in the higher end of this range. The initial tail consists of a 17 square inch rudder and a 36 square inch elevator, but these values are easily adjustable in the future to accommodate for control requirements.

The location of the tail is also important, as it has to be far enough from the center of mass of the aircraft to generate a sufficient moment for controllability. Based on initial sizing estimates, the preliminary design consisted of a 30 inch moment arm between the aerodynamic center of the tail and the center of gravity of the aircraft.

4.2.4 Power System Sizing and Selection.

The last key aircraft component that had to be properly sized was the power system. The wing was designed before the power system, so the responsibility of the power system was simply to generate enough speed within the 10 foot runway to achieve takeoff velocity. However, the power system is also where a large portion of the aircraft weight comes from, so selecting a properly sized motor was crucial to optimal performance. The thrust equations detailed in Equations 3,4 and Figure 13 were used to analyze power systems, and it was determined that a 14 volt motor combined with a 10 or 11 inch propeller would be able to achieve the desired thrust of around 30 N.

$$T_R = \frac{W}{L/D}$$

Equation 3: Thrust required for level, unaccelerated flight

$$P_R = \sqrt{\frac{2W^3 {C_D}^3}{\rho S {C_L}^3}}$$

Equation 4: Power required for level unaccelerated flight

Dynamic Thrust Equation
F = thrust (N), d = prop diam. (in.), RPM = prop rotations/min., pitch = prop pitch (in.), V_0 = propeller forward airspeed (m/s)

Expanded Form:

$$F = 1.225\frac{\pi(0.0254 \cdot d)^2}{4}\left[\left(RPM_{prop} \cdot 0.0254 \cdot pitch \cdot \frac{1min}{60sec}\right)^2 - \left(RPM_{prop} \cdot 0.0254 \cdot pitch \cdot \frac{1min}{60sec}\right)V_0\right]\left(\frac{d}{3.29546 \cdot pitch}\right)^{1.5}$$

Simplified Form:

$$F = 4.392399x10^{-8} \cdot RPM\frac{d^{3.5}}{\sqrt{pitch}}(4.23333x10^{-4} \cdot RPM \cdot pitch - V_0)$$

Gabriel Staples, 2013. http://electricrcaircraftguy.blogspot.com/

Figure 13: Equations for Determining Generated Thrust

4.3 Performance Calculations and Estimates

4.3.1 Power System Performance Estimates

The first aspect of performance analyzed was the power system. Table 5 details full performance estimates for various motor and propeller setups that were considered. It was ultimately decided to opt for a 1250 kV motor and a 10 inch diameter propeller, however the propeller can easily be switched out to fine tune performance before technical inspection.

Volts	kV	Diameter(in)	Pitch(in)	RPM	Thrust(N)	Watts	m/s prop
14	1100	10	5	15400	20.49	229.01	16.30
14	1100	10	6	15400	24.40	272.68	19.56
14	1100	11	5	15400	28.61	319.69	16.30
14	1100	11	6	15400	34.06	380.66	19.56
14	1250	10	5	17500	28.12	314.24	18.52
14	1250	10	6	17500	33.02	369.02	22.22
14	1250	11	5	17500	39.25	438.67	18.52
14	1250	11	6	17500	46.09	515.15	22.22

Table 5: Power Performance Estimates

4.3.2 Aerodynamic Performance Estimates

Simulations were performed in order to predict the lift and drag generated by the aircraft over the operable range of angles of attack. Most of these simulations were performed through SolidWorks CFD analysis (Figure 14).

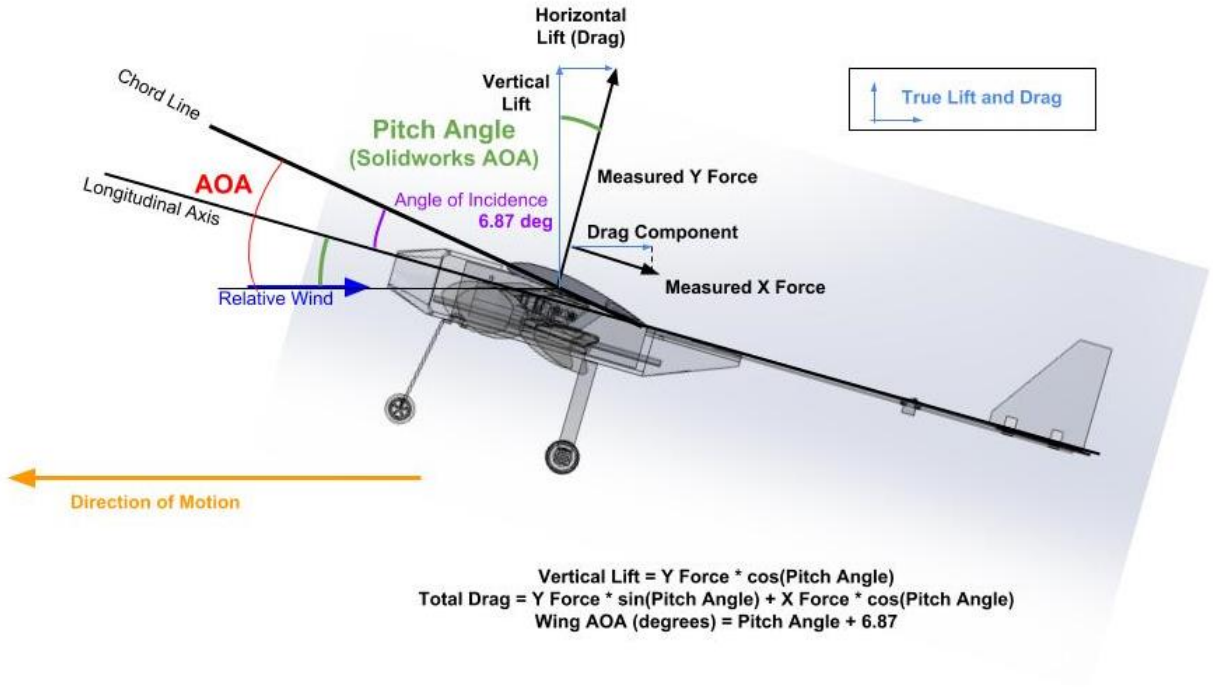

Figure 14: SolidWorks CFD Analysis Method

These simulations provided a wide range of data for the predicted aircraft performance, detailing the impact of angle of attack and flap angle on lift and drag. These values of lift and drag were used for all subsequent performance calculations.

Simulations were run on a clean wing (no flaps) to determine the angle at which the wing will stall (Table 6). Critical angle of attack was found to be close to 17 degrees, which confirms expected airfoil performance (Figure 15).

Wing Lift vs AOA (no flaps)
Wing Angle of Incidence: 6.87 degrees

Pitch Angle (degrees)	Wing AOA (degrees)	Y Force (N)	Vertical Lift (N)
0	6.87	10.04	9.97
2.5	9.37	20.12	16.02
5	11.87	20.01	19.58
7.5	14.37	22.77	22.06
10	16.87	24.55	23.49
12.5	19.37	21.99	20.75

Table 6: Clean Wing Lift vs AOA

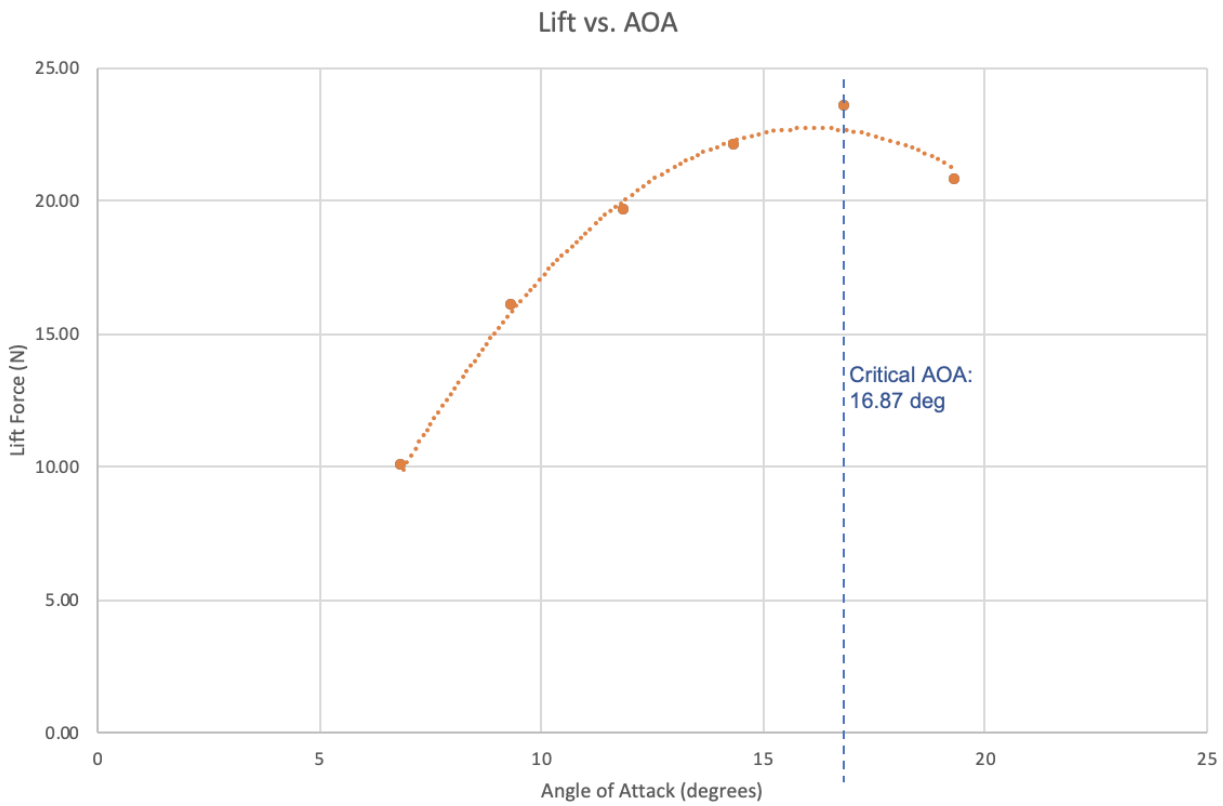

Figure 15: Critical Angle of Attack

Flap angle was then varied with angle of attack to determine the flap angle and AOA for maximum lift on takeoff. Maximum lift on takeoff occurs at 12.5 degree pitch angle with near 10 degree flap deflection (Table 7) (Figure 16).

Lift (N)	Angle of Attack (deg)						
Flap Angle	**0**	**2.5**	**5**	**7.5**	**10**	**12.5**	**15**
0	12.837	19.04	25.038	24.593	29.604	34.54	33.388
2	14.195	19.287	26.002	25.381	29.944	34.495	33.441
4	14.438	19.879	26.869	26.076	30.304	34.577	33.738
6	15.149	20.528	27.54	26.281	30.72	34.934	34.886
8	15.725	21.073	27.931	26.745	31.296	35.619	35.352
10	16.294	21.457	28.753	27.177	32.209	36.812	36.734
12	17.35	21.927	29.633	27.506	32.073	36.397	36.553

Table 7: Lift Based on AOA and Flap Setting

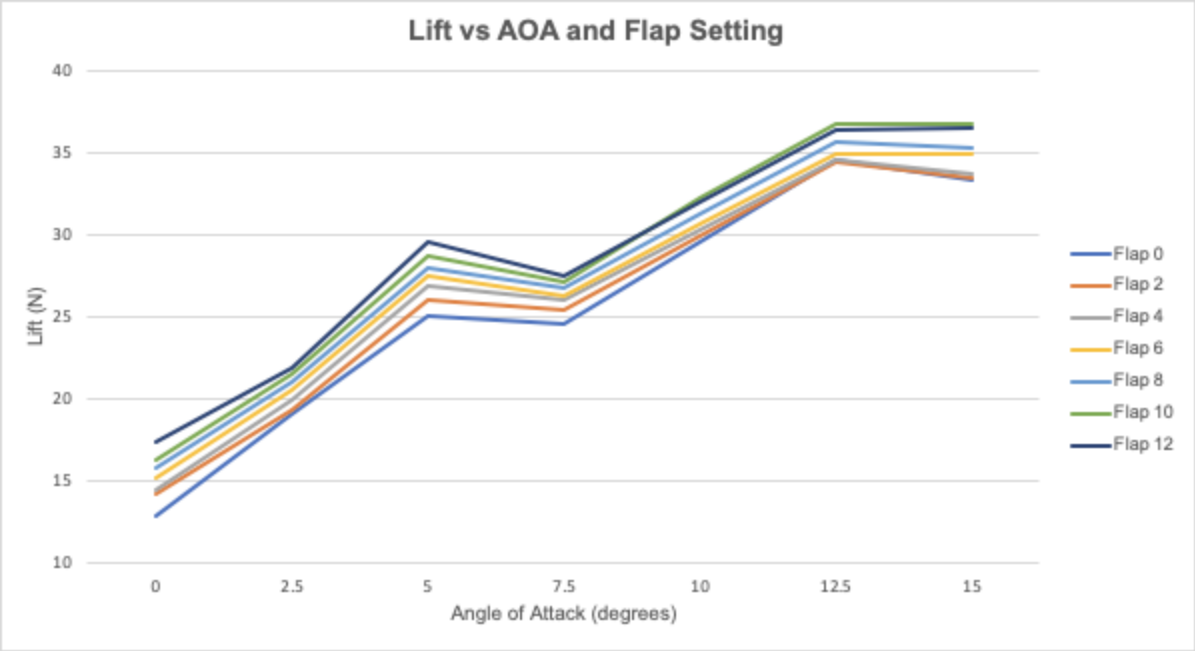

Figure 16: Lift vs AOA at Various Flap Settings

Drag was also calculated for each AOA and flap setting. Drag increases with AOA and increased flap angle (Table 8) (Figure 17).

Drag (N)	Angle of Attack (deg)						
Flap Angle	**0**	**2.5**	**5**	**7.5**	**10**	**12.5**	**15**
0	4.874	6.094	5.832	7.337	8.723	10.29	11.589
2	5.056	6.167	6.01	7.537	8.848	10.317	11.68
4	5.194	6.31	6.202	7.747	9.034	10.458	11.872
6	5.319	6.496	6.381	7.883	9.198	10.653	12.403
8	5.443	6.659	6.517	8.039	9.4	10.918	12.673

10	5.584	6.784	6.758	8.186	9.656	11.355	13.19
12	5.811	6.959	7.005	8.38	9.67	11.254	13.162

Table 8: Drag Based on AOA and Flap Setting

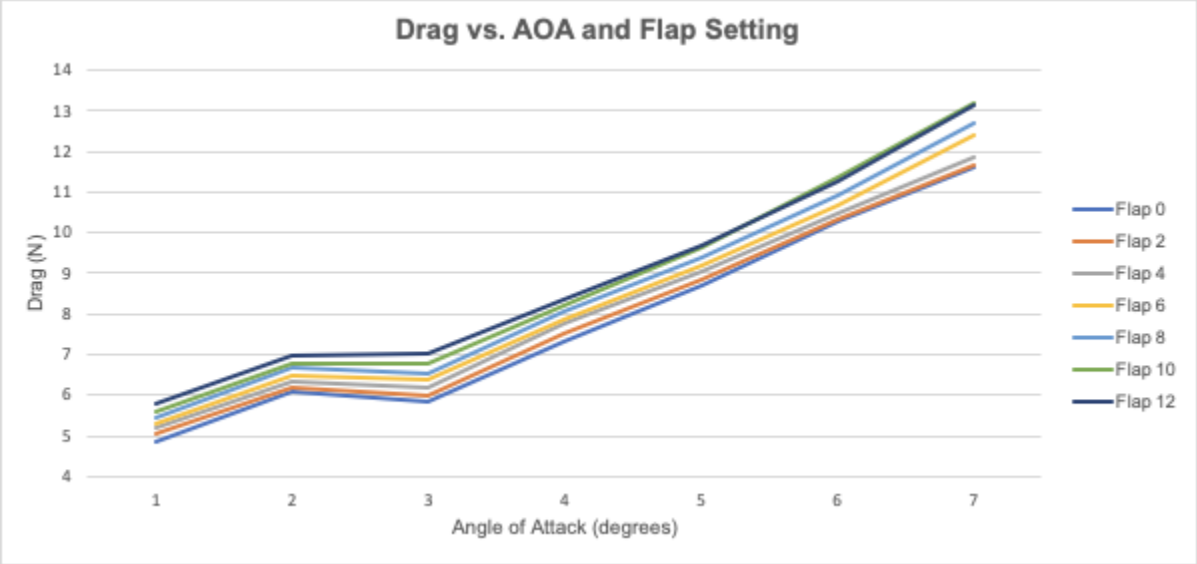

Figure 17: Drag Based on AOA and Flap Setting

4.3.3 Mission Flight Time Calculations

Per mission requirements, for the first two missions the competition course had to be completed within 5 minutes. To verify that this was achievable given the preliminary design, the course length was estimated given the provided geometry, and the average flight speed was calculated. For an average calculated flight speed of 15 m/s and a course length of conservatively 10000 feet, the calculated flight time was 203 seconds. Given the amount of buffer between this and the time restriction, this confirmed that timing would not be an issue for any of the flight missions. Mission 3, due to the additional lap needed to drop the fourth store, will take approximately 281 seconds, but will still be well within the required time limit of 10 minutes.

4.3.4 Takeoff Distance Calculations

Before proceeding with design refinements and construction, it had to be confirmed that the aircraft was be able to takeoff within the 10 foot runway ramp. To determine whether or not this was feasible, Equation 5 was used to calculate the takeoff ground roll.

$$S_{LO} = \frac{1.44W^2}{g\rho S c_{L,max}\{T - [D + u_r(W - L)]avg\}}$$

Equation 5: Takeoff ground roll distance

It was determined that the aircraft had a takeoff ground roll distance of 8.9 feet, providing confidence that the design was capable of taking off within the 10 foot runway ramp.

4.3.5 Drop Mechanism, Wing Folding Mechanism, and Radome

The drop mechanism, wing folding mechanism, and radome were designed to have minimal impact on the aerodynamics of the aircraft. By using precise construction techniques and fine sanding, the goal was to minimize drag and weight wherever possible. Remote controllability was a key part of both mechanisms, as all three mechanisms had to be controlled remotely. An electronic speed controller was used to finely control servo motors which controlled all three systems.

4.4 Mission Model

The first two flight missions of this competition consist of the aircraft taking off from a 10 foot long ramp and then performing three laps around the specified course within the 5 minute time window. For the first mission, the aircraft has no payload and for the second mission, the radome is attached. The third flight mission consists of completing 4 laps within 10 minutes, where one attack store is dropped on each lap. The average speed of the designed aircraft far surpasses the minimum speed required to complete these missions within the specified time. Aircraft controllability throughout the climbing, turning, and descending flight was an important part of the mission model. Remote control flight simulator RealFlight 8 was used to simulate individual parts of the mission. An aircraft was loaded with custom parameters to mimic the anticipated aircraft performance. Takeoff and climb are viewed as the most challenging parts of these missions, so they were repeatedly practiced to ensure consistent success. The different turns required to complete the course were also practiced, and the aircraft performs well across these maneuvers. These simulations were used to predict the overall aircraft performance for the three flight missions, and to allow pilots to become familiar with flight characteristics.

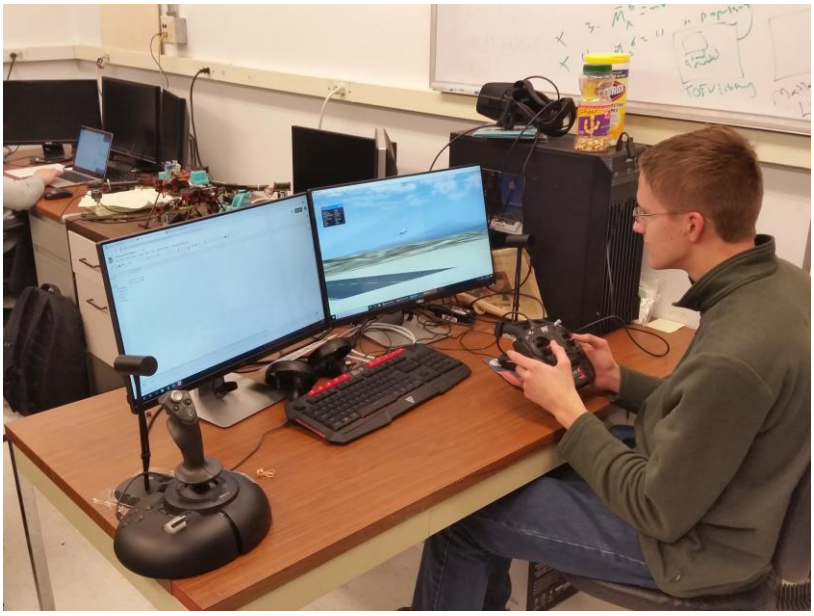

Figure 18: Flight Simulator Testing

5. Detailed Design

5.1 Design Structure and Dimensional Parameters

Between the preliminary and final stages of this project, there were no major alterations required for the aircraft. The specifications of the aircraft matched the specifications of the preliminary CAD model and are described in the following table.

Wingspan (in.):	52.125	**Rudder Area (in^2):**	14.5
Wing Chord (in.):	10.0	**Vertical Stabilizer Area (in^2):**	33.4
Wing Area :	521.25	**Weight (unloaded) (lbs):**	4.4
Aspect Ratio:	5.21	**Weight (radome) (lbs):**	0.22
Elevator Area	33.5	**Weight (stores) (lbs):**	0.8

(in^2):			
Horizontal Stabilizer Area (in^2):	51	**Total Length (in.):**	50.1

Table 9: Final Parameters

5.2 Material Characteristics and Capabilities

The fuselage is constructed of extruded polystyrene, chosen for its adaptability, durability, and cost. This material allowed for easy hot wire cutting and sanding for optimal aerodynamics. Furthermore, the foam was taped over in many places to further reduce drag on the aircraft. In order to reinforce the foam, circular carbon fiber spars and rods were used for the wing and tail construction. The rods' excellent strength-to-weight ratio enabled a sturdy aircraft that could accommodate the extra weight and moment of the wing folding and attack store mechanisms. The stabilizers and control surfaces of the tail were constructed from foam core poster board Aluminum was utilized for the landing gear due to the high strength-to-weight ratio, as well as the low cost and availability. Aluminum is significantly lighter than other similar metals, and is strong enough to support the aircraft entirely.

5.2.1 Fuselage Structure

The main structure of the plane consists of extruded polystyrene, hot wire cut into an aerodynamic shape, reinforced with a carbon fiber spar running from the front of the fuselage to the rear. A second carbon fiber spar then extends from the rear of the fuselage and connects the components of the tail. The carbon fiber offers the fuselage rigidity while the elastic properties of the foam were used to dampen vibrations and absorb energy from rough landings or minor crashes. The fuselage is also held together with hot glue, which is extremely effective in holding the foam together and limits buckling or cracking in the foam.

5.2.2 Landing Gear Structure

The landing gear structure is composed of a 1 inch by 1/16 inch aluminum bar bent into a symmetric shape with elastic bands connecting axles of the structure. The form analysis in MATLAB indicated that the aluminum is strong enough to prevent buckling and the elastic band is used to apply a force to the base of the landing gear which reduces the overall deflection. The landing gear is tied into the carbon fiber backbone of the fuselage to prevent the impact of landing from tearing through the foam parts of the fuselage.

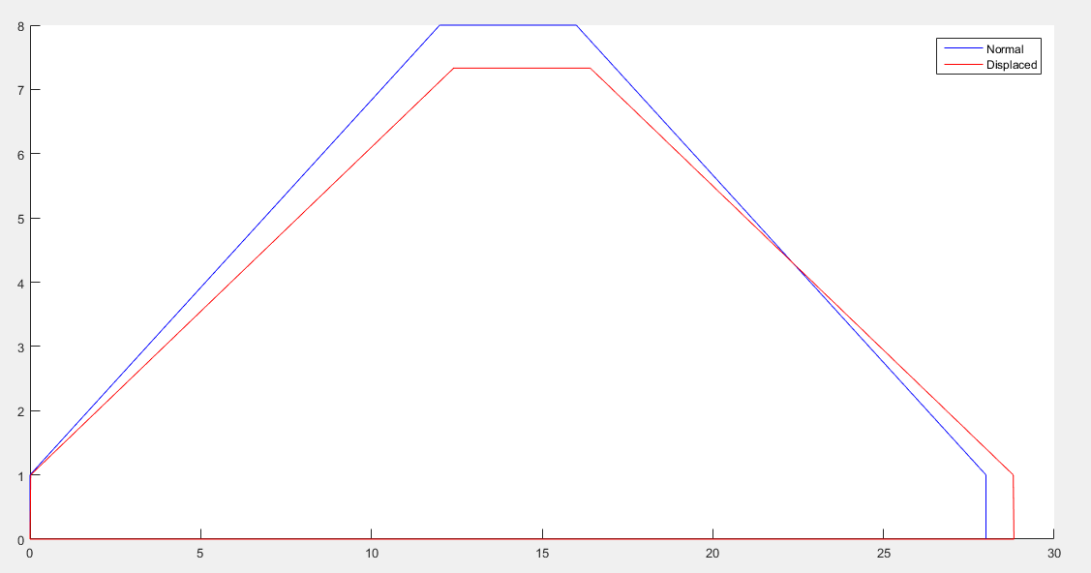

Figure 19: FEM analysis of the landing gear using MATLAB

Figure 20: Main Landing Gear

5.2.3 Wing Structure

The wing of the aircraft is composed of Extruded polystyrene foam that has been hot wire cut into the shape of a NACA 4412 airfoil with a 10inch chord. The polystyrene foam is reinforced with multiple 8mm diameter carbon fiber spars running through the center of the wing. To mount the wing to the fuselage to wing down rods are mounted in the fuselage and elastic bands are strapped over the wing in parallel and crisscross fashion. The use of elastic bands to hold down the wing allows for a flexible connection between the fuselage and the wing. The flexibility of the joint was needed because it was realized that

there was a high probability that this wing would be involved in a crash. With an elastic joint, a large amount of the kinetic energy would be absorbed, minimizing the forces induced in other components when angular displacement occurs at this joint. Such a connection also allows for greater serviceability of the electronics in the fuselage and faster repair time in the event of a crash. The wing hold-down rods are composed of round carbon fiber tubes that are mounted into the sides of the fuselage. The hold-down rods are then tied into the carbon fiber square tube that runs the length of the fuselage.

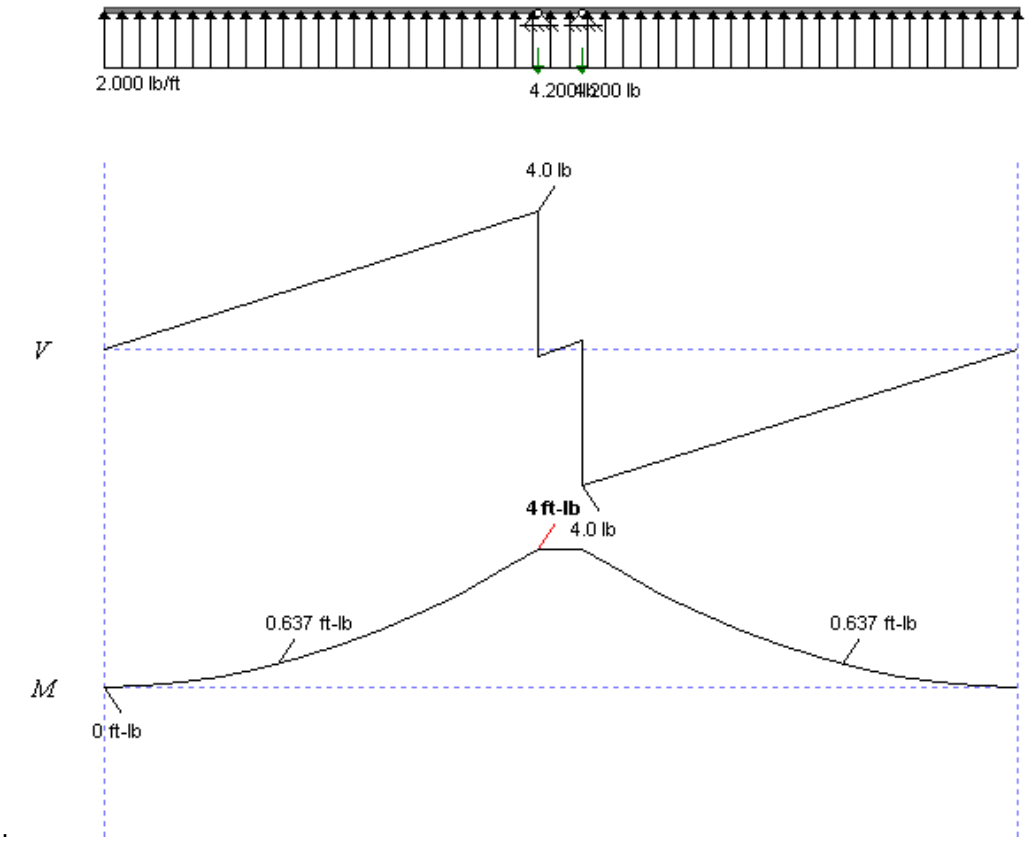

Figure 21: Shear Moment Diagram for Wing

5.2.4 Tail Structure

The tail of the aircraft is conventional in nature, with a single vertical stabilizer and a two-piece horizontal stabilizer. The servos to control the rudder and elevator were then mounted to the carbon fiber rod forward of the tail, using 3D-printed PLA mounts. The tail and rudder were then mounted onto the carbon fiber rod using 3D-printed brackets at the rear of the aircraft. Both stabilizers, as well as the horizontal and vertical stabilizer are constructed out of foam core board. They are then reinforced with carbon fiber and steel rods to resist bending moments. The horizontal stabilizer is symmetrical across the airframe, with approximately a half inch gap in the middle to allow for clearance with the carbon fiber rod.

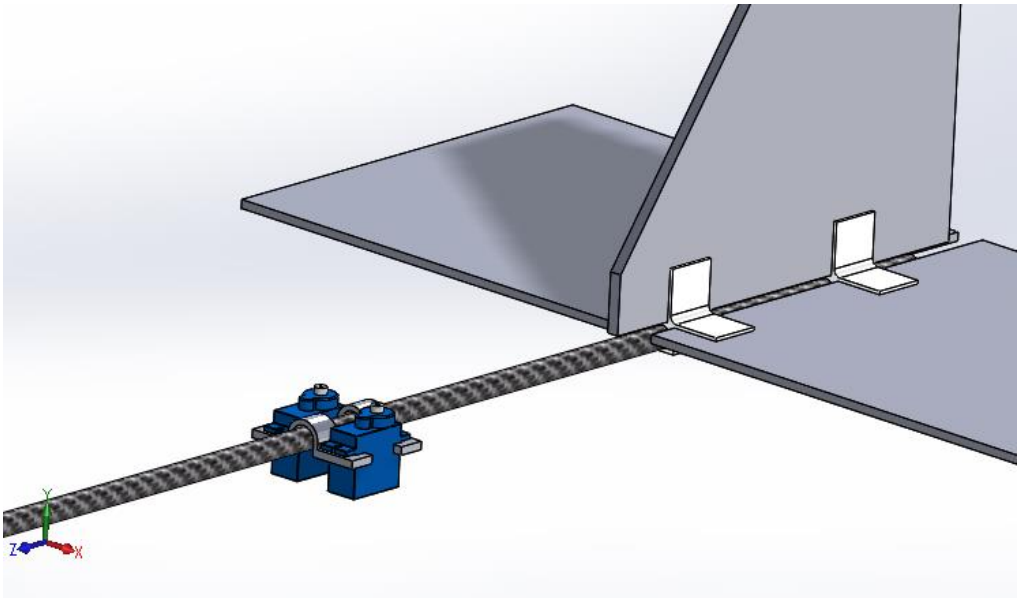

Figure 22: Tail and Control Servos

5.3 Subsystem Design and Integration

5.3.1 Wing Fold Mechanism

With the choice of the wing folding mechanism, it was initially hypothesized that a servo-driven pin would be utilized to mechanically lock the folding sections in place. Initial testing of the 3D-printed mechanism, however, proved this unnecessary. The screw and shaft of the mechanism proved to serve as an effective mechanical locking mechanism in and of themselves. Without the moment produced by the servo to rotate the shaft, there are no means for the screw to move translationally with reference to the shaft, meaning that the screw is locked in place and thus the wing folding sections are locked in place.

With this, the final wing folding design is as follows: a servo rotates a screw-like mechanism, which pulls and pushes two mounts. As the mechanism rotates in, the screw forces the two mounts together, bringing the wingtip up until it is flush with the fixed component. A hinge further connects the stationary wing to the moving wing, resisting the force of the lift in flight and holding the sections of the wings together.

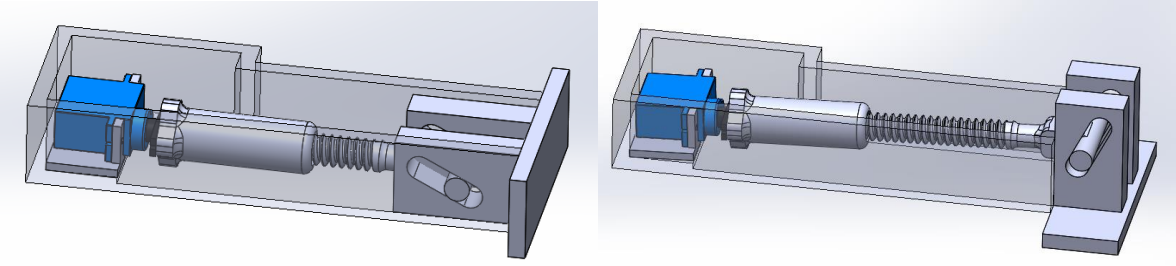

Figure 23: Models for the Wing Fold Mechanism

5.3.2 Drop Mechanism

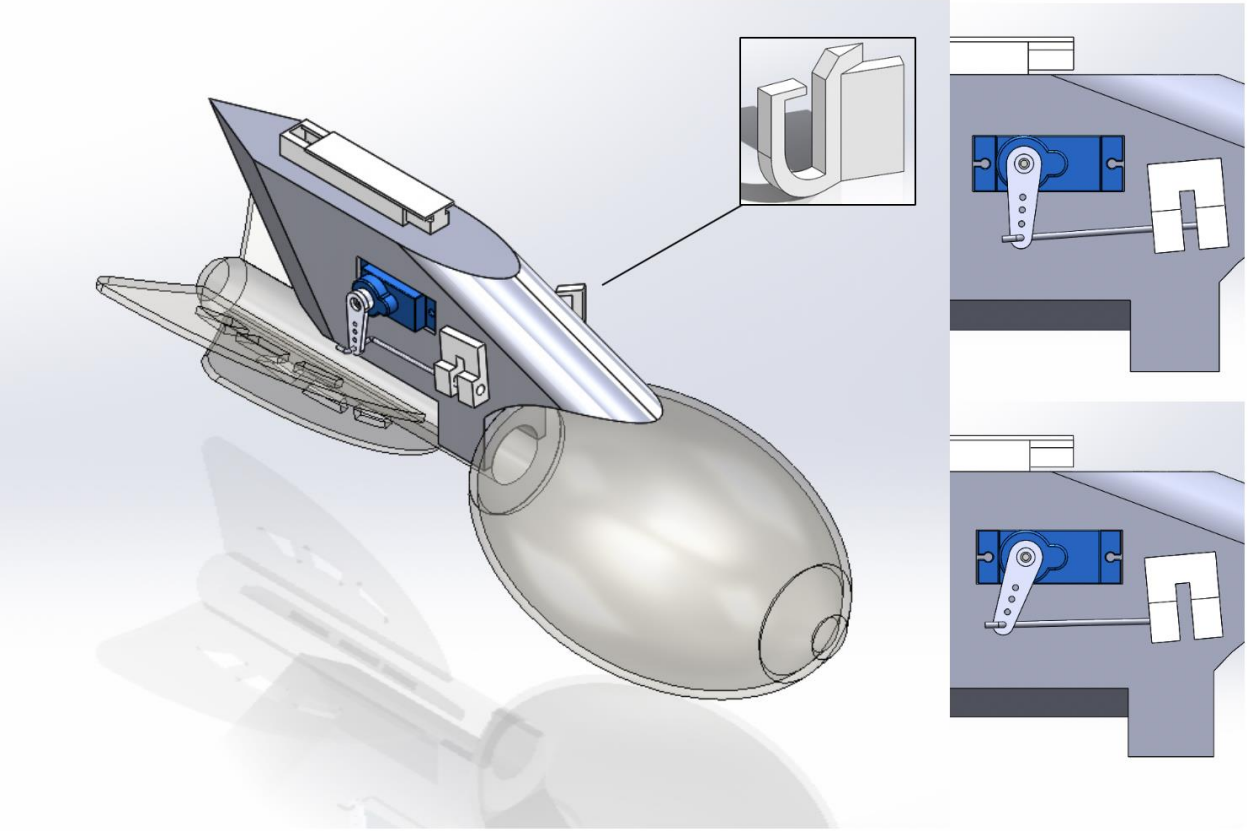

Figure 24: Drop Mechanism

To ensure that the drop mechanism operates consistently, it must be as simple as possible. The selected design minimizes complexity while providing adequate torque resistance to secure the store in place. The drop structure consists of a pylon hardpoint which supports the store and the release mechanism. Each pylon is attached to the wing by a sliding 3D-printed track for ease of replacement. A rubber band is used to secure the store against the hardpoint.

The loading of all 4 stores in the minimum possible time is important to scoring, and load time is minimized by this design. A rubber band secured inside a 3D-printed bracket by a servo-actuated pin is wrapped under the store and attached to a 3D-printed hook to mount the store to the pylon. Once in flight, a servo on each pylon withdraws the pin into a hole in the bracket, forcing the release of the rubber band and allowing store separation. The hook is designed to prevent the rubber band from separating with the store (Figure 24).

5.3.3 Radome

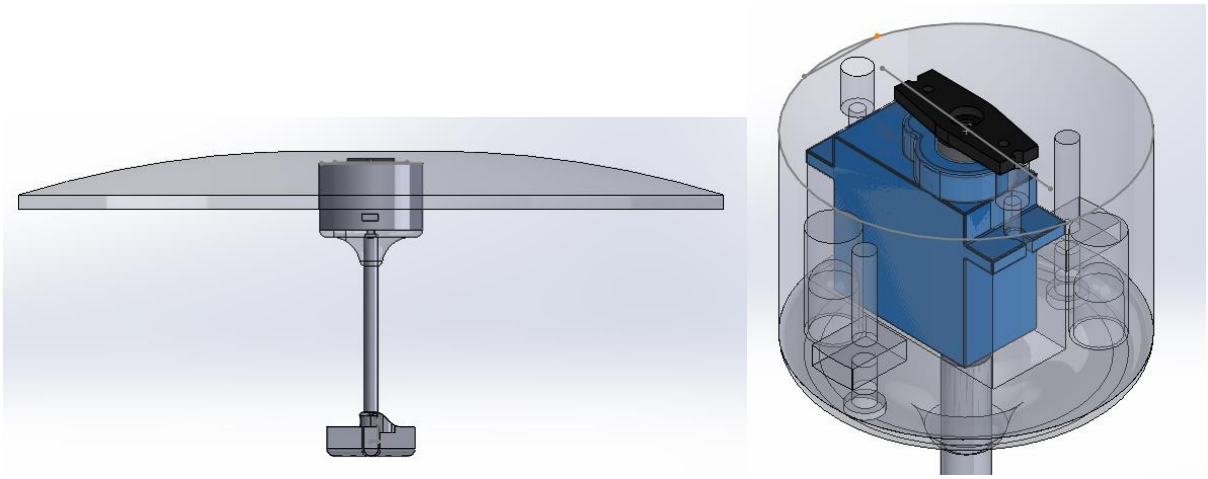

Figure 25: Radome and Control Servo

The radome is constructed out of a polystyrene dish mounted to a carbon fiber rod via a 3D-printed PLA servo housing. It is anchored directly to the polystyrene fuselage via a housing which it is screwed into. Additionally, the radome is able to rotate on command by utilizing a 9 gram servo which mounts to a plate that rotates the disk. Since the radome is quite large in diameter and must rotate, it induces quite a lot of drag. To mitigate this, the disk tapers radially outwards from the center to create a more aerodynamic profile, while having the added benefit of weight reduction. The placement of the servo within the radome also reduces the stress on the servo, as the moment arm between the point of application of the net drag force and the servo is reduced.

5.3.4 Control Surfaces

The control surfaces consist of four features: ailerons, flaps, elevators, and rudder. The flaps are positioned along the entirety of the trailing edge of the main (stationary) wing section and are articulated by servos embedded in the underside of the wing and control rods. The ailerons are positioned on the folding sections of the wing, articulated in the same manner as the flaps. Both the flaps and ailerons are attached to the wing with hinge pins, mechanical components consisting of a single hinge and a cylindrical pin on either side. Respectively, the flaps and ailerons are 13.5 inches in width and 3 inches in

depth, and 6 inches in width and 2.5 inches in depth.

The elevators and rudder each exist along the entirety of the trailing edge of the horizontal and vertical stabilizers. These are attached to the tail proper by small plastic hinges embedded in the foam surfaces of the control surfaces and tail proper. These two control surfaces are approximately a third of the size of the horizontal and vertical stabilizers, respectively.

5.4 Weight and Balance

	Weight (lbs)	CG_x (in)
All Stores	5.15	0
Store 1,2,3	4.9625	0.642
Store 2,3	4.775	0
Store 3	4.5875	0.490
No Stores	4.4	0

Table 10: Store Weight and Balance

5.5 Drawing Packages

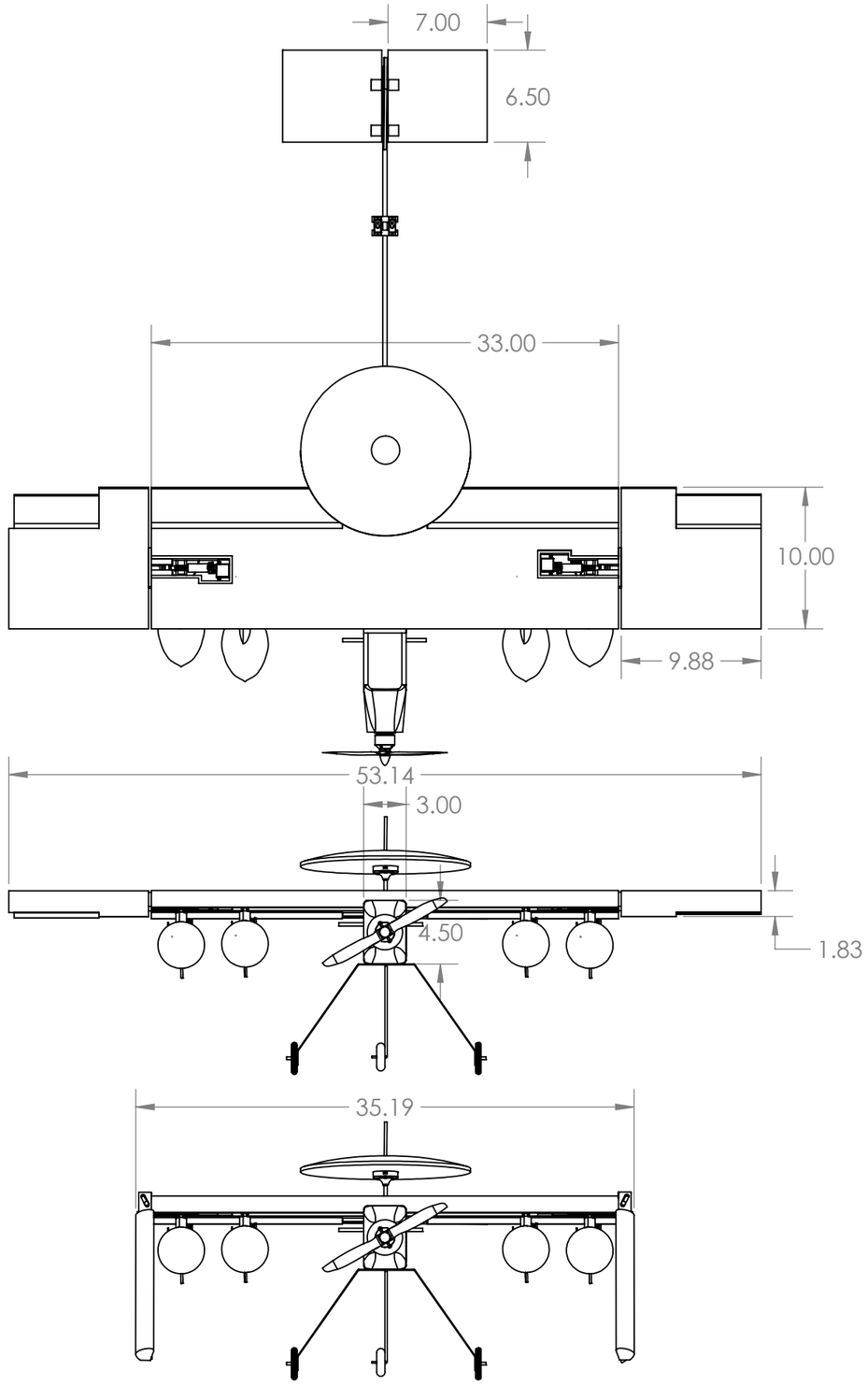

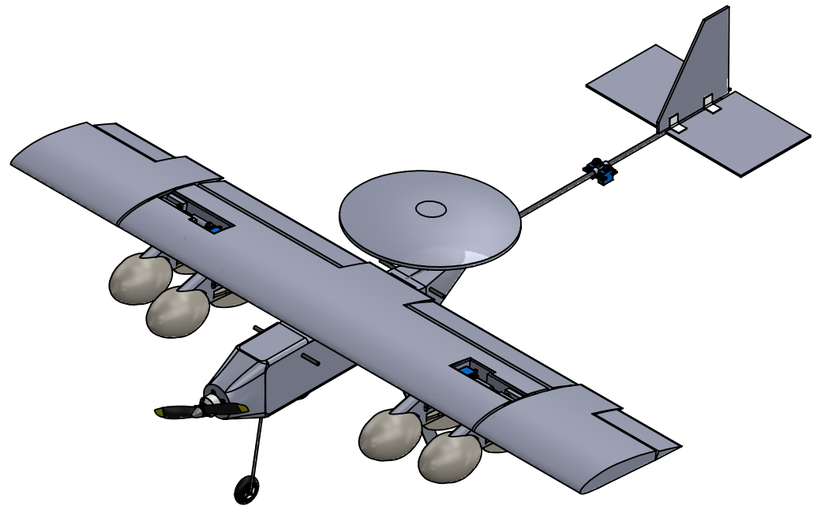

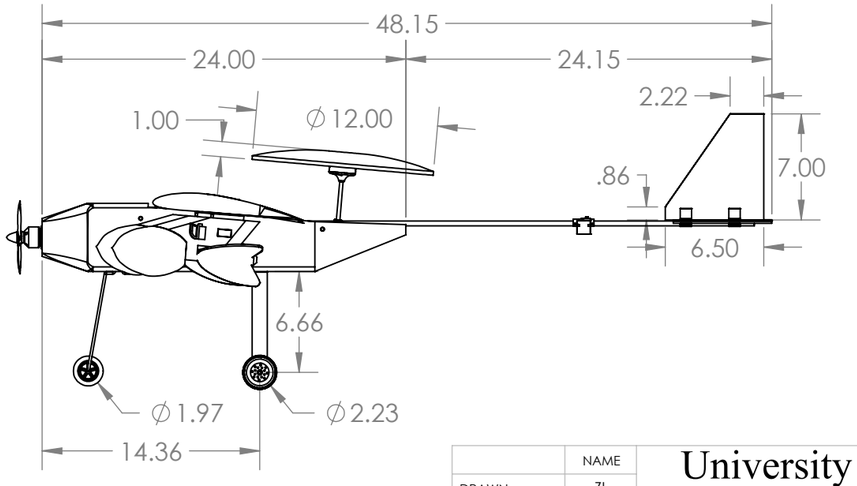

	NAME
DRAWN	ZL
CHECKED	
ENG APPR.	
MFG APPR.	
Q.A.	
COMMENTS:	

University of Washington
Design, Build, Fly Team at the University of Washington

TITLE: Squawk 7700

SIZE B | Three View Drawing | REV

SCALE: 1:10

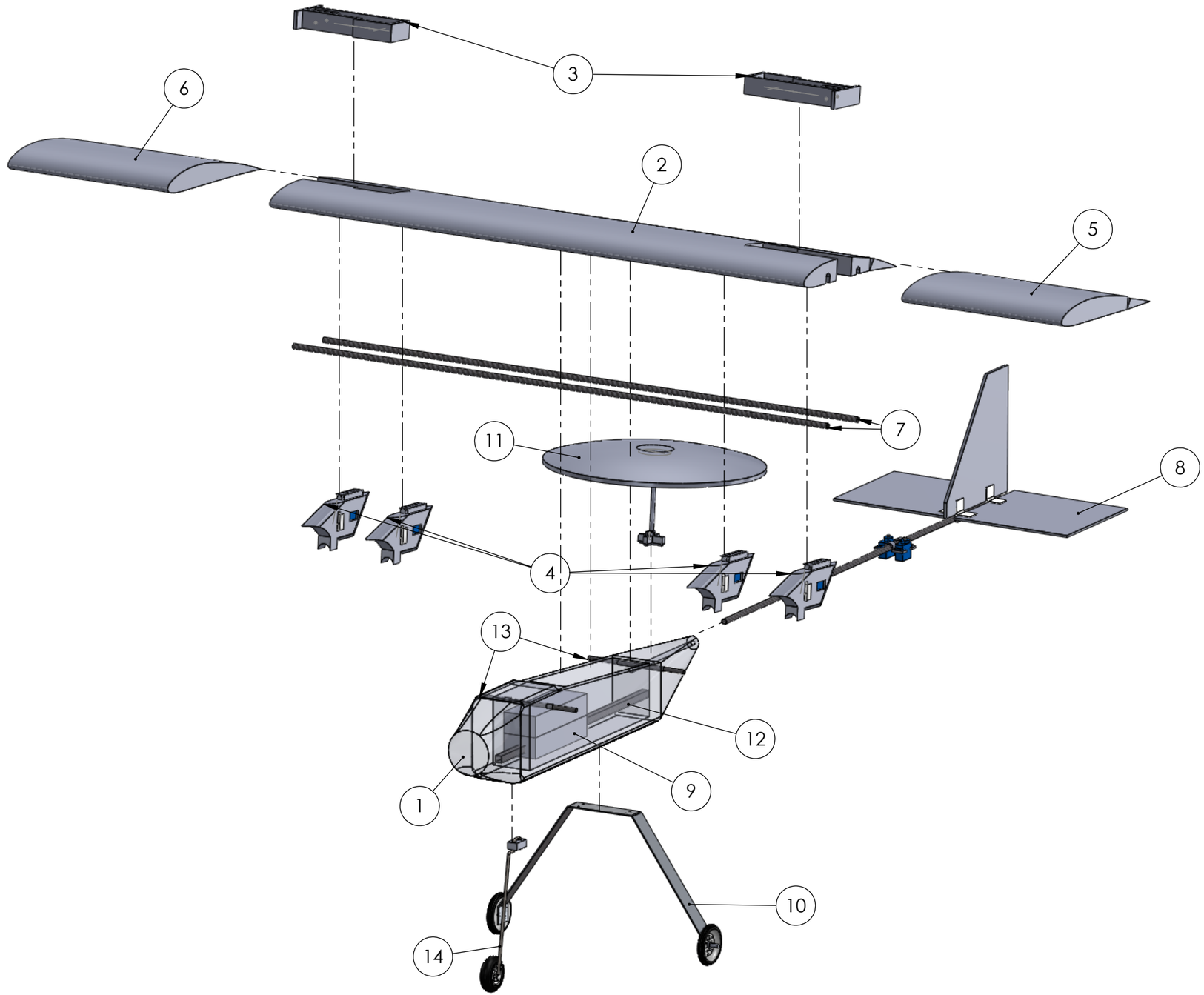

ITEM NO.	PART NUMBER	QTY.
1	Fuselage Frame	1
2	Main Wing	1
3	Fold Mechanism	2
4	Rubber Band Drop Mechanism	4
5	Wing Ext Left	1
6	Wing Ext Right	1
7	Wing Spar	2
8	Tail Section	1
9	Battery	2
10	Rear Gear	1
11	Radome	1
12	Fuselage Structure	1
13	Fuselage Spar	2
14	Forward Gear	1

	NAME
DRAWN	ZL
CHECKED	
ENG APPR.	
MFG APPR.	
Q.A.	
COMMENTS:	

University of Washington
Design, Build, Fly Team at the University of Washington

TITLE: Squawk 7700

SIZE B | Structural Arrangement | REV

SCALE: 1:6

ITEM NO.	PART NUMBER
1	Fuselage Frame
2	Battery
3	Landing Gears
4	Wing
5	Folding Mechanism
6	Drop Mechanism
7	Radome
8	Tail Section
9	Motor & Propler

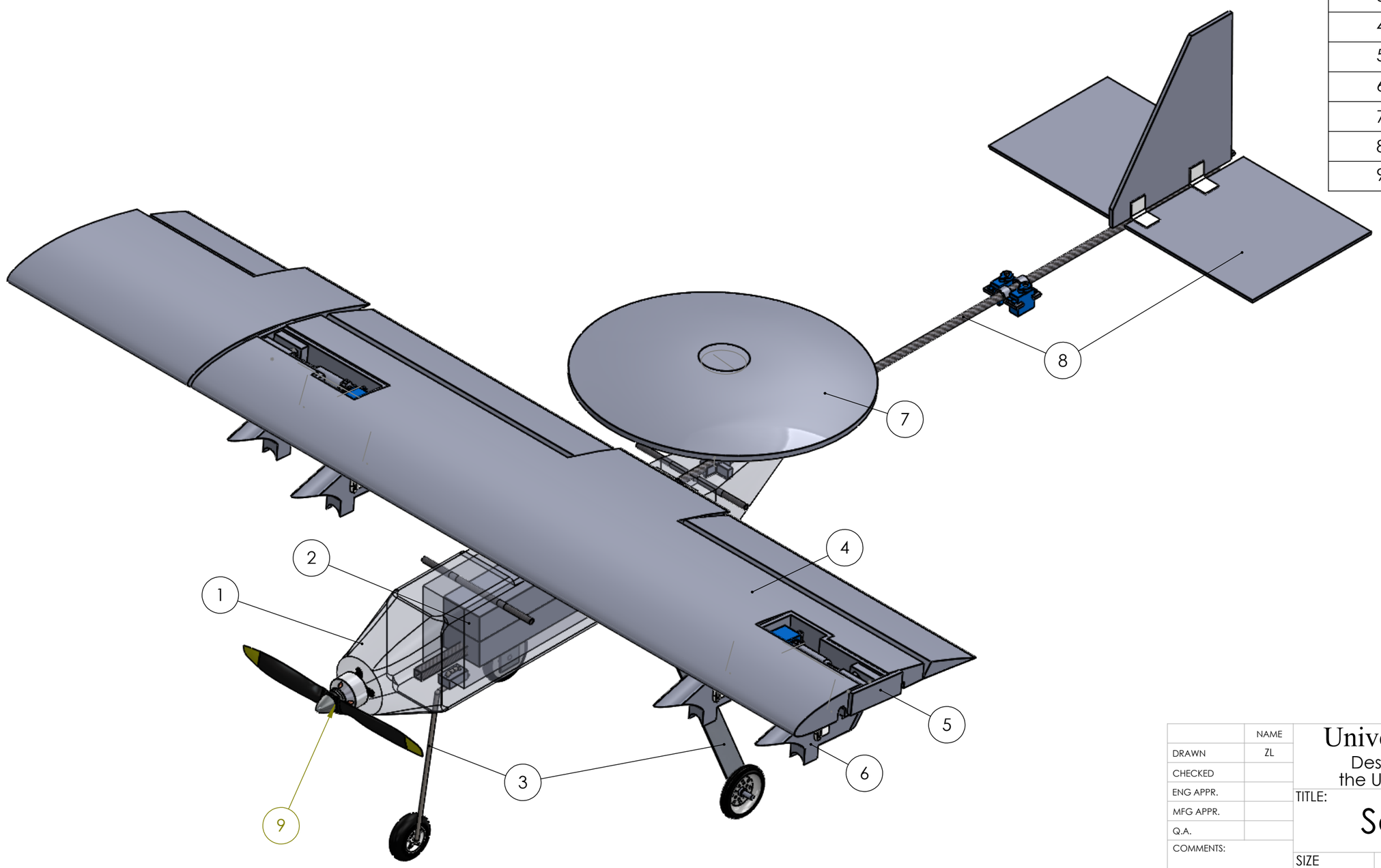

	NAME
DRAWN	ZL
CHECKED	
ENG APPR.	
MFG APPR.	
Q.A.	
COMMENTS:	

University of Washington
Design, Build, Fly Team at the University of Washington

TITLE: Squawk 7700

SIZE B | Systems Layout | REV

SCALE: 1:4

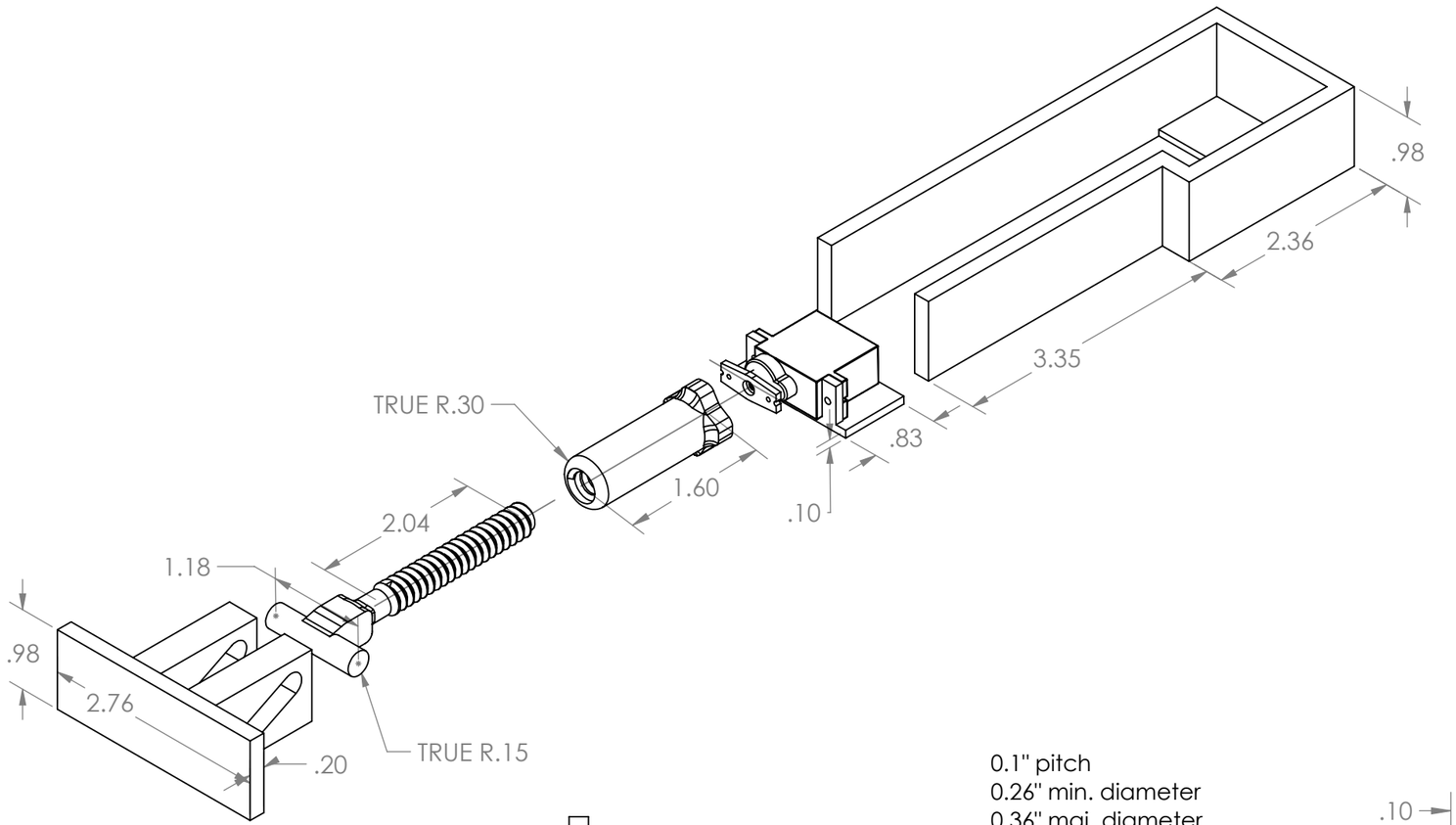

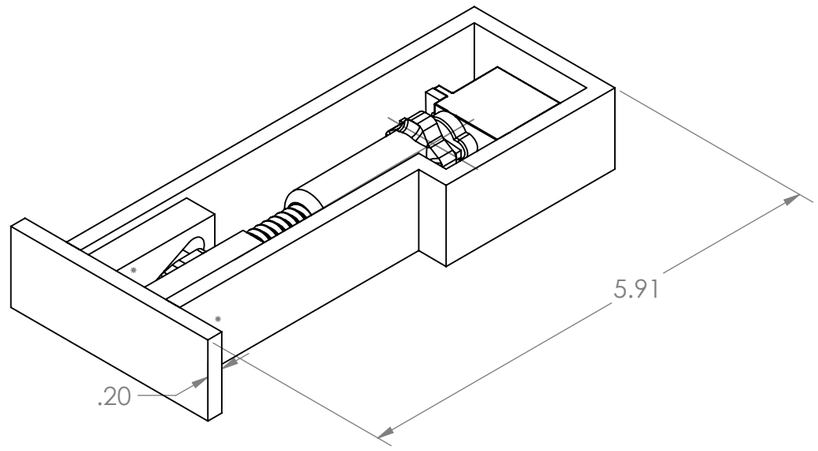

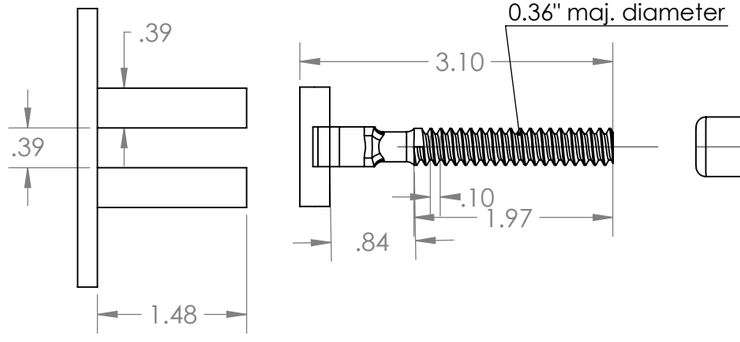

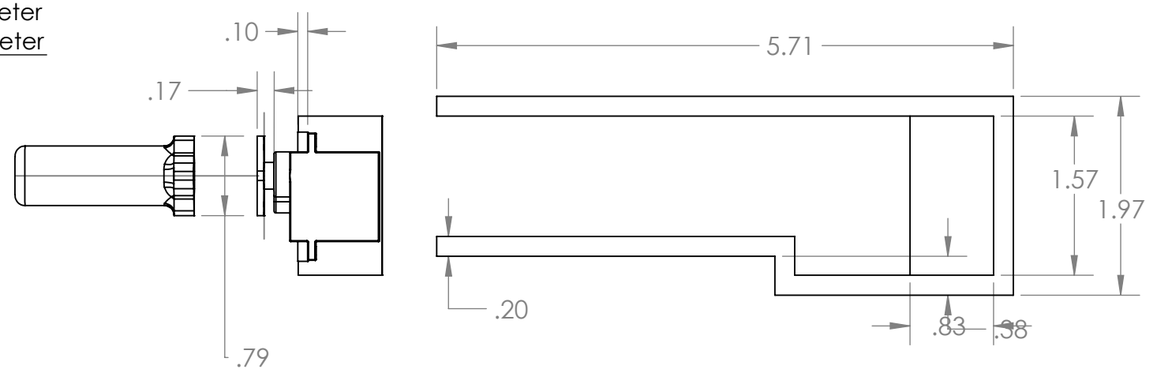

		UNLESS OTHERWISE SPECIFIED:		NAME	DATE
		DIMENSIONS ARE IN INCHES TOLERANCES: FRACTIONAL ± ANGULAR: MACH ± BEND ± TWO PLACE DECIMAL ± THREE PLACE DECIMAL ±	DRAWN		
			CHECKED		
			ENG APPR.		
			MFG APPR.		
		INTERPRET GEOMETRIC TOLERANCING PER:	Q.A.		
		MATERIAL	COMMENTS:		
NEXT ASSY	USED ON	FINISH			
APPLICATION		DO NOT SCALE DRAWING			

TITLE:

SIZE | DWG. NO. | REV

B WingFoldAssm

SCALE: 1:1.5 | WEIGHT: | SHEET 1 OF 1

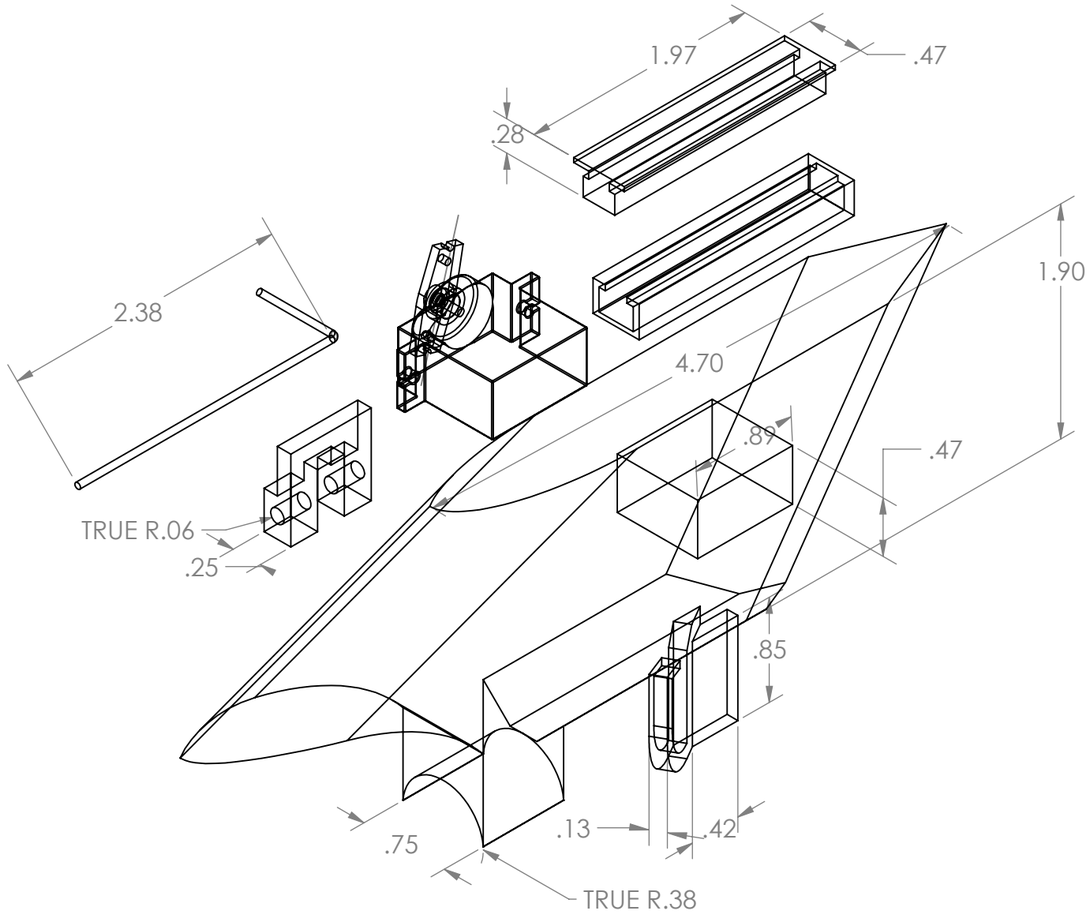

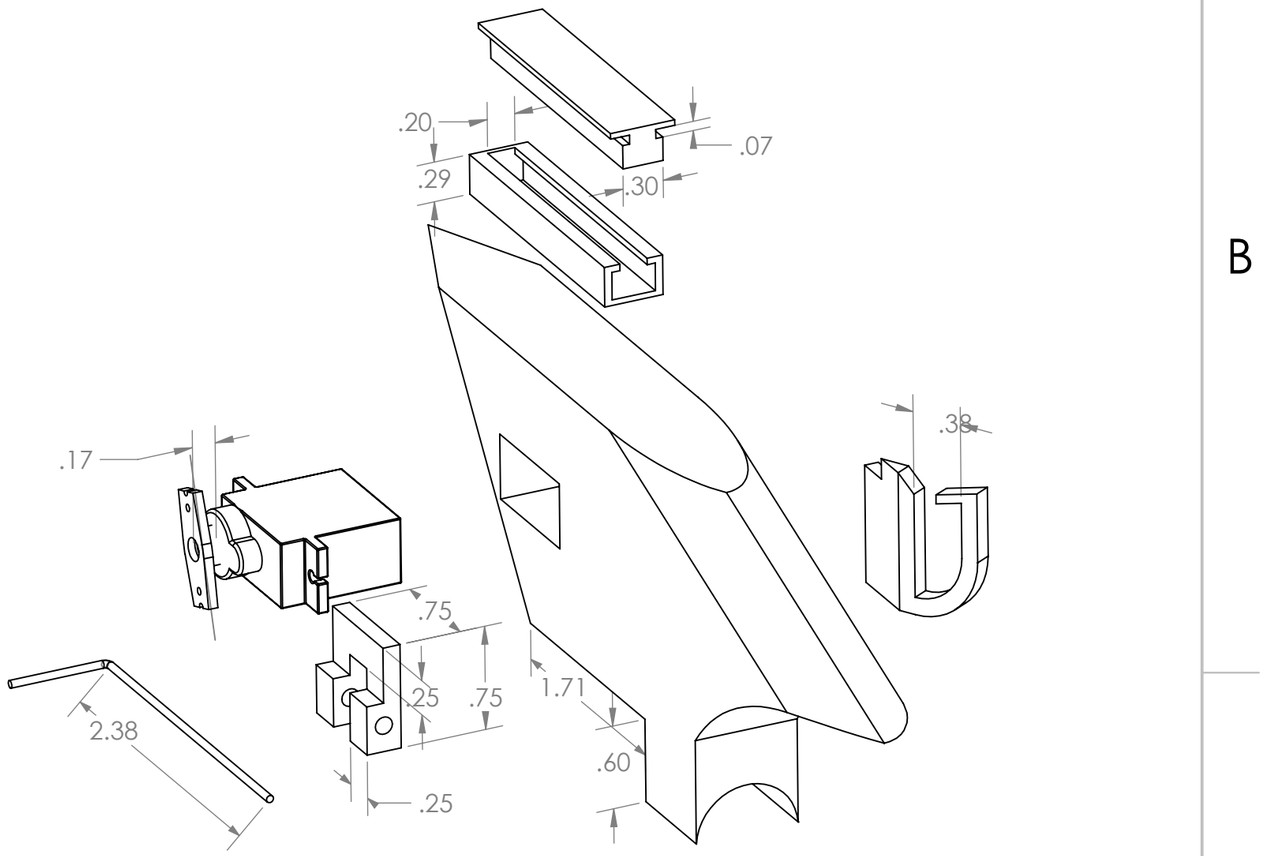

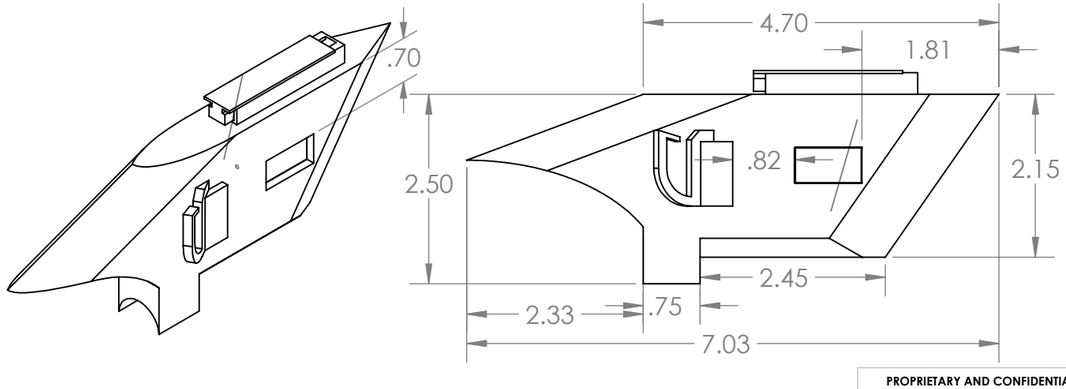

NEXT ASSY	USED ON	FINISH
APPLICATION		DO NOT SCALE DRAWING

UNLESS OTHERWISE SPECIFIED:

DIMENSIONS ARE IN INCHES
TOLERANCES:
FRACTIONAL ±
ANGULAR: MACH ± BEND ±
TWO PLACE DECIMAL ±
THREE PLACE DECIMAL ±

INTERPRET GEOMETRIC TOLERANCING PER:

MATERIAL

	NAME	DATE
DRAWN		
CHECKED		
ENG APPR.		
MFG APPR.		
Q.A.		

COMMENTS:

TITLE:

Rubber Band Drop Mechani

SIZE	DWG. NO.	REV

SCALE: 1:1	WEIGHT:	SHEET 1 OF 1

6. Manufacturing Plan

6.1 Manufacturing Methods Considered

6.1.1 Wings

Fiberglass wings were considered but not selected due to complexity and weight. Polystyrene foam wings were instead selected, and constructed by cutting polystyrene with a hot wire cutter. First, stencils were cut from plywood, based on the SolidWorks model of the aircraft. These stencils were cut using a laser cutter to ensure accuracy. After attaching the stencils to large blocks of foam, cuts around the stencils were made to ensure that the resulting wing matched the same dimensions as the CAD model. The wing was separated into four parts in the construction process. First, the wing section was cut using the stencils as guides, ensuring that the wings matched the SolidWorks design. The wings were sanded for shape precision. Then, sections for the flaps and ailerons were measured and marked, as well as sections that would support the wing folding mechanism.

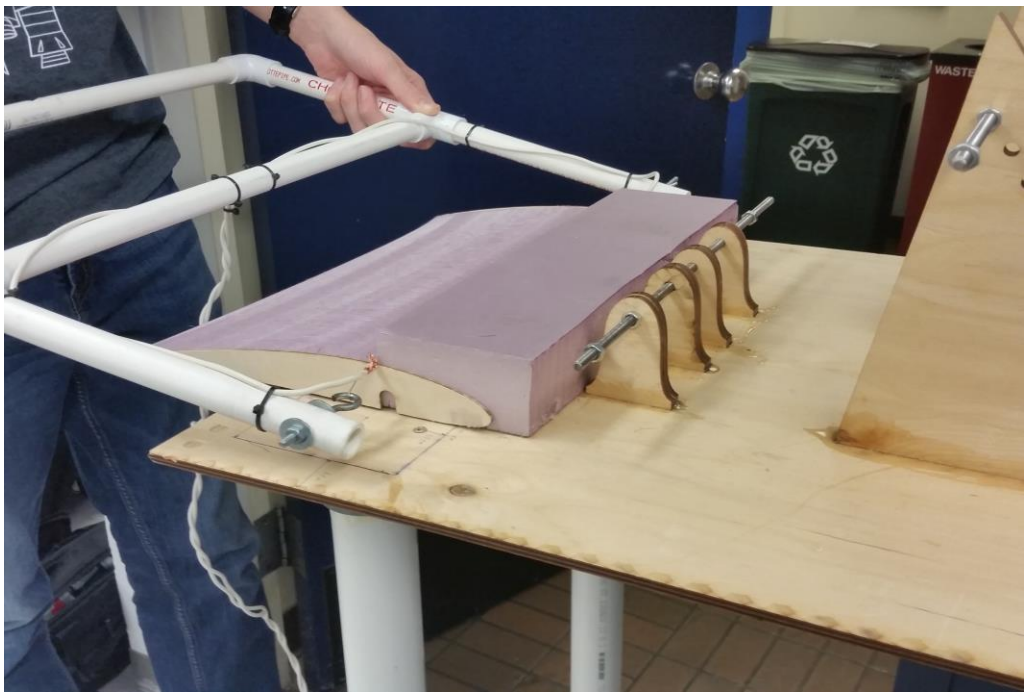

Figure 26: Hot wire cutting a wing

6.1.2 Wing folding mechanism

The components of the wing fold mechanism were 3D-printed, ensuring that they matched the specifications from the design. The mechanisms for each wing were 3D-printed into rectangular mounts, then matching holes were cut out of the wing sections where the mounts needed to be attached. Hot glue was used to hold the mounts to the inside of the wing, preventing the mounts from falling out of place. Holes were then drilled through the inside corners of the mechanism frames to accommodate for servo wires. Servos were then attached with screws to the mounting mechanism.

6.1.3 Fuselage

Stencils for the fuselage were first laser cut out of plywood. Initially, fiberglass and balsa were considered as possible fuselage materials but were rejected in favor of polystyrene foam, which has superior durability, lesser weight, and easier replacement. A hot wire cutter was used to cut sections of polystyrene around the stencils, resulting in several parts that were connected together with hot glue to form the nose and rear of the fuselage. Three rectangular sections were then measured and cut out of foam to form the sides and base of the fuselage, then a section was removed with a knife where the fuselage would connect to the rear landing gear. A large hole was also drilled into the rear of the fuselage where the tail spar would connect, then mounts for rubber bands holding the wing to the fuselage were secured on the sides.

6.1.4 Landing gear

A tricycle gear was selected as it was the most stable configuration, allowed for maximum pitch angle on takeoff. The main gear is just aft of the most aft CG, while the nose gear is positioned just forward of the leading edge of the wing.

a. Front gear: aluminum rod identical in diameter to front gear coiled 5 times using vice grips

b. Front gear: aluminum rod identical in thickness and width to selected rear gear bent with vice grips

c. Rear gear: 2 aluminum rods identical to selected front gear bent into strut shape specified by design requirements using vice grips

d. Rear gear: solid aluminum bar of dimensions (¾ in wide 8 in high) with rubber bands, anchored by bolts, strung between the struts.

6.1.5 Tail section

Extruded polystyrene foam board was considered due to its structural strengths but was not chosen due to the difficulty of constructing a piece of dimensions required. The decision was made to use foam board, which greatly reduced the difficulty of constructing the tail and reduced weight. The surfaces of the

tail were carefully measured and cut out using a knife, separated into control surfaces (rudder and elevators) and fixed surfaces for each stabilizer.

6.1.6 Drop Mechanism

For the drop mechanism, the possibility of 3D-printing the pylons was considered alongside the use of laser-cut stencils and foam hot wire cutting. The weight of plastic, however was deemed too great, and so the pylons were constructed primarily of foam. Stencils were used to guide rough wire cutting of the pylons, which was followed up by finetune sanding allow for close matching of the store to the pylon. The hole for the servo was carefully cut out using a knife and the detailed rubber band hook and wire guide were 3D-printed and hot glued to the pylon.

6.2 Manufacturing Methods Selected

6.2.1 Wings

Manufacturing of the wing was perhaps the most labor-intensive part of the build phase. Three different hot wire cutters were constructed for different purposes. One was set up to work like a bandsaw with a level table and guides, while the others were made to be handheld 33 inch and 18 inch size cutters. Pieces of 2 inch thick polystyrene foam were cut with the table setup to dimension before being modeled to general size with the handheld cutters before final shaping and profiling was done with sandpaper of various grits.

Flaps and other control surfaces were cut out of the final profiled wing with a combination of knife and drill to ensure proper size and shape. All servos and other control devices were attached with hot glue (chosen for its ease of use and compatibility with foam since epoxy is known to melt it) into recessed areas of the wings (for maximum aerodynamic airflow).

Primary structural and electrical components were added into grooves that were cut out during the shaping phase (i.e. carbon-fiber spars and servo wiring).

After wing finalization, masking tape was used to laminate the final structure in order to increase durability and smoothness.

6.2.2 Wing fold mechanism

The wing fold mechanism was constructed out of 3D-printed material and consisted of several parts. The parts included a case designed to be mounted into the fixed wing, a screw to drive the mechanism, and a corresponding case for the moving sections so that the mechanism is connected to both sections. Once the parts were printed, sections of the wing were cut out, and the cases were placed and secured into the wing with hot glue. The screw was then attached to the cases, and the servos were connected to

the mechanism. The mechanism for each wing was then tested, and the servos were fully secured to the wing following successful tests.

6.2.3 Fuselage

The main body of the fuselage was cut from 2 inch polystyrene foam into 6 main pieces. The central piece is composed of three main pieces while the nose and tail sections are made with a combination of polystyrene blocks and hot glue. Several holes were cut out of the fuselage by knife or drill with the purpose of inserting a carbon-fiber spar or landing gear mount brackets.

The motor mount of the fuselage was manufactured with 2 different wood plates for mounting, one on the inside face of the fuselage and one on the outside in order to counter the twisting moment of the motor and anchor it into the nose better.

6.2.4 Landing gear

A square aluminum strut was selected for the rear gear. The strut was bent into shape manually using vice grips. The wooden bracket was aligned above the top section, and two small wood screws were screwed into drilled holes. A larger hole was drilled into the center of an adjacent side on the bracket, and a carbon fiber rod roughly ¼" in diameter was glued into that hole. Small rubber wheels were attached to the vertical area of strut at the bottom via holes drilled in the area, and an axle and screws were placed to hold the wheel. A square hole with dimensions corresponding to the horizontal area of the bracket was cut into the fuselage via X-Acto knife, and the bracket was inserted rod-first into the whole, and zip-tied to the central longeron from the opposite side of the fuselage, open for accessibility.

The front gear was relatively simple. The steel rod was bent into shape via vice grips, a wheel was placed directly on the strut at the horizontal bottom section, constrained on one side by a set screw and on the other side by the vertical section. A hole was drilled into the forward section of the fuselage at the strut angle, and the strut was inserted into the hole and zip-tied to the longeron.

6.2.5 Tail section

The horizontal and vertical stabilizers were constructed out of paper-faced foam board due to the relative ease of construction and replacement. The foam board is also very lightweight, which helps prevent the aircraft from becoming tail heavy. Printed stencils were used to outline the stabilizers, and a knife was used to precisely cut out the sections separately. The horizontal stabilizer was cut out in two sections, as they were attached on separate sides of the tail spar. The elevators and rudder were cut directly out of the stabilizers and then reconnected in place with plastic hinges.

A bracket capable of holding the tail surfaces and the tail spar was then 3D printed and glued to the tail spar. Servos for the rudder and elevator are mounted to the spar further forward in a housing, and then 1/16 inch control rods are run from the servos to control horns on each surface.

6.2.6 Drop mechanism

The pylons for the stores were cut from 1 inch polystyrene foam using laser-cut wood stencils, then sanded to the precise desired shape. A hole was cut for the servo, which was embedded using hot glue. The release bracket, hook, and attachment slide were then attached to the foam surface using hot glue. A steel wire was cut to the proper length for the release pin and attached to the servo arm.

6.3 Manufacturing Milestones

6.3.1 Manufacturing chart

Table 11 below displays the manufacturing schedule of components and systems in the aircraft. As shown, only electrical components, store systems, and landing gear are still in production, as those components are being refined prior to competition. Landing gear structure and CAD took longer than expected for design refinements, but did not delay further scheduling.

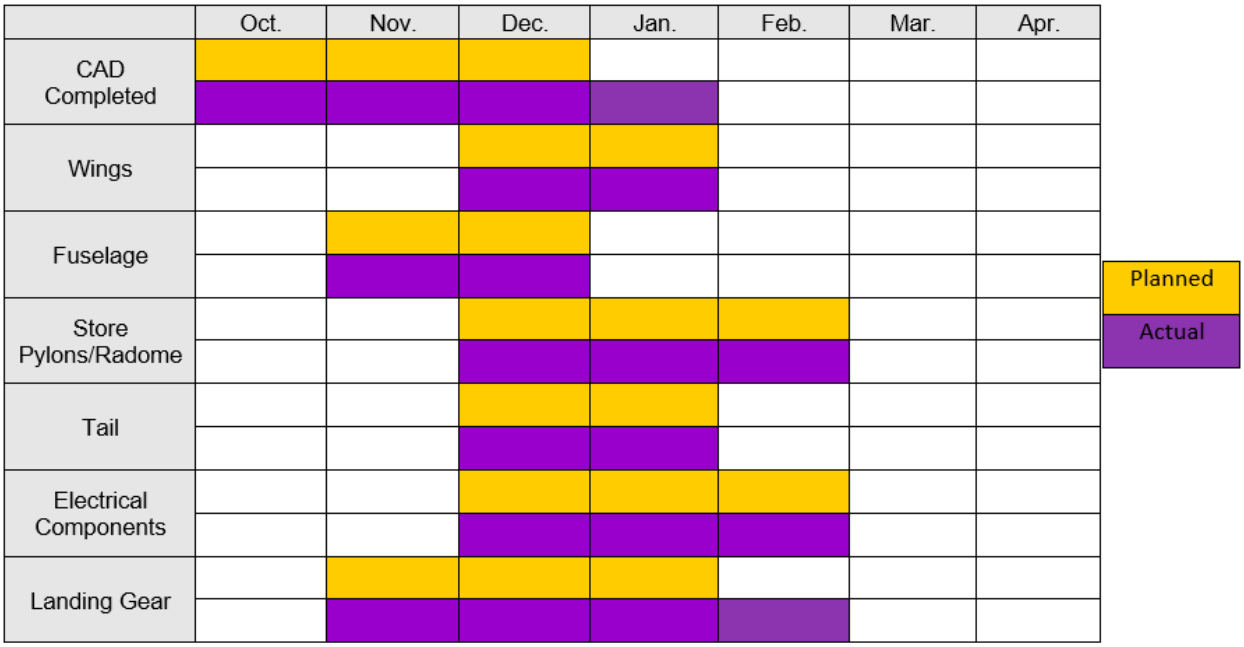

Table 11: Manufacturing timeline chart

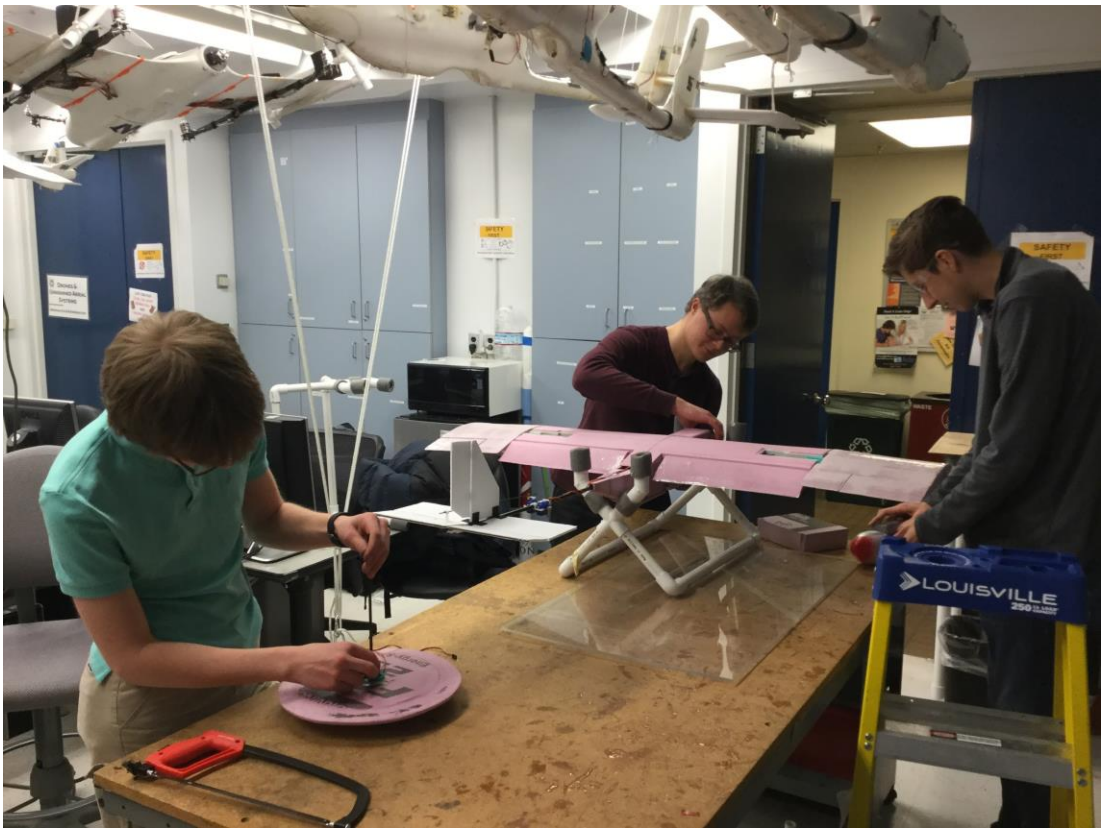

Figure 27: Team construction meeting, assembling radome and drop mechanisms

University of Washington DBF Testing Schedule	October				November				December				January				February				March				April			
Component																												
Aerodynamics																												
Propulsion																												
Structures																												
Ground Testing																												
Flight																												
Preliminary Design																												
Intermediary Designs																												
Competition Design																												

Table 12: Component Testing Plan

Table 12 identifies the testing schedule, starting with static testing of components and small-scale component prototypes in October and continuing through flight test, which is projected to conclude in early April.

7.1 Test Objectives and Schedule

Component testing began in early October, first testing small-scale iterations of drop mechanisms and wing fold designs. Initial system testing included heavily use of the RealFlight 8 flight simulator to verify structural integrity and proper flight characteristics. Wing and tail testing occurred largely concurrently with propulsion testing, and predominantly utilized the RealFlight 8 simulator. Once an approximate max gross weight of the aircraft was identified, propulsion testing began. A large variety of motor combinations were tested, focusing on approximately a 1250 kV motor in the 300-650 Watt range. A variety of propeller sizes ranging from 9 inch to 12 inch were tested. The aircraft was tested in a variety of flight phases, with various load configurations to determine the optimum loadout for competition. Initial simulated aircraft iterations were used to determine the flight performance of various configurations. After this step, the structural layout was verified through simulated mission flights. Wingtip tests were used to confirm the structural integrity of the design. This test simulates the maximum wing loading the aircraft will undergo while in flight. The plane is lifted at the wingtip, which induces a moment through the wing. This validated spar strength, and verified proper center of gravity in various, mission-dependent loadouts. These test results then were used to determine necessary design modifications before a tangible aircraft was constructed.

7.2 Flight Test Schedule and Flight Plan

Flight testing was conducted once ground testing had verified the specific components for use. The initial aircraft conducted several flights to verify proper functioning of components, control surfaces, and accurate takeoff performance. Once the aircraft reliably and consistently flew while in an empty configuration, pylons were installed and further tests were performed with the stores and radome installed. Minor modifications were made to the pylons by shaving them and reprofiling the leading edge to further reduce drag. After the aircraft repeatedly had demonstrated adequate performance fully loaded, testing of the radome rotation and independent drop mechanism began. The aircraft flew a scaled down version of the competition track and one store was dropped independently on the downwind leg. Repeatability was emphasized in this particular test to verify that the aircraft could reliably drop one store independently. The aircraft flew several additional flights in its final configuration under a variety of weather conditions to ensure sufficient control authority in crosswinds, enough power under high angle of attack or gusty situations, and proper functioning of all servos throughout the flight profile.

7.3 Test and Flight Checklists

Date	Objectives
02/01/2019 (First Flight)	This test verified the feasibility of the conceptual design and tests control system concepts for each prototype. No payloads were flown.
02/15/2019 (Second Flight/Pylons and Stores Static)	This test simulated the entire competition missions and verified the detailed compiled aircraft design, stores and radome will be present, but in static condition only.
02/26/2019 (Planned) (Stores/Radome Dynamic)	This test will verify that the improvements made perform as expected. Mission simulation will again be conducted, stores will be dropped and the radome will rotate.
03/01/2019 (Planned) (Competition Takeoff)	This test will test the capability of the competition-ready model, with a competition-spec ramp takeoff. Adjustments will be determined.
03/21/2019 (Planned) (Final Verification)	This test will verify that the adjustments made meet the team's expectations. This test will also serves as a final practice run for the pilot.

Table 13: Flight test schedule

Table 13 describes the outline of each flight and objectives that need to be achieved. To ensure adequate performance and satisfaction of all testing parameters, checklists were developed. During flight testing, a flight log, as seen in Figure 28 ensured the aircraft flew safely and in an organized fashion.

Design, Build, Fly at the University of Washington Flight Log

Note: Please upload this flight log to the online folder pertaining to the corresponding aircraft.

Flight #: _____ Take-Off Time: _____:_____ AM / PM

Date of Flight: _____/_____/_____ Flight Duration: _____ Min _____ Sec

Battery Used: _____ CG Location: _____

Total Takeoff Weight: _____ lb. Weather: _____

Wind Conditions: _____ mph, coming in from N / NE / E / SE / S / SW / W / NW

Pre-Flight Checklist:

- o Motor securely fastened
- o Wing securely fastened
- o Empennage securely fastened
- o Landing gear lubricated and rolling smoothly
- o Payload onboard and secured
- o Main battery connected
- o Propeller free of obstructions
- o Power on
- o Full control surface deflection
- o Full motor speed control

Post-Flight Checklist:

- o Power off
- o Main battery disconnected
- o Aircraft inspected for damage

Purpose of Flight:

_____

_____

_____

Payload:

_____

_____

_____

Notes:

_____

_____

_____

_____

_____

Figure 28: Flight test log

8. Performance Results

The aircraft was tested at a field near the University of Washington campus. The aircraft executed the flight tests with specific parameters in mind. First, the aircraft's airworthiness was determined. After the aircraft was comfortably stable, it executed several maneuvers to define the flight characteristics. These including banking and pitching maneuvers, stalls, and low level flying to understand the ground effects on the aircraft.

8.1 Performance of Key Subsystems

8.1.1 Battery Performance

The endurance of the main battery was tested by flying the aircraft at cruising speed and recording the time until the power was exhausted. The lasting time was measured for the attack configured aircraft, the aircraft in reconnaissance configuration, and the empty aircraft, as seen in Table 14. Mission 1 requires the empty aircraft to fly at a moderate throttle setting for 4 min. As demonstrated in the endurance test, the battery and motor selected are capable of providing sufficient power for mission 1, with a safety factor of nearly 200%. Mission 2 requires the reconnaissance-loaded aircraft to fly 3 full laps. Since the radome does not add much weight, and has a minimal aerodynamic penalty, 7.5 minutes should allow a wide margin of error for successful mission completion. The aircraft carries 4 attack stores, and as such will require 4 laps for successful mission completion, dropping one store per lap. Even with a heavier gross weight to begin, 6.75 minutes allows for a wide margin of error.

Empty Load	**9.00 min**
Reconnaissance Mission	**7.50 min**
Attack Mission	**6.75 min**

Table 14: Battery endurance

8.1.2 Attack Store Drop Mechanism

Static tests were initially performed to verify that the servo motors could be activated to successfully individually release the attack stores. Each pylon was tested individually multiple times in order to ensure the capabilities and reliability of the drop mechanism. Key to the success of these tests was the alignment of the rods to allow for quick store loading. Static tests were successful, and provided confidence to progress to in flight drop testing.

To test the drop mechanism in flight, a series of shortened test flights were performed, in which the aircraft would get up to flight altitude and immediately begin individually dropping the stores. There were

initially some issues with accurately timing the store drops, but this was quickly remedied by minor tweaks in the mounting procedure and increased pilot training.

8.1.3 Radome Testing

The radome is mounted on a rod that is directly on top of a 360 degree servo that can rotate freely. Initially it was static tested in order to ensure that it could continually rotate while remaining stable about the axis of rotation, and these tests proved successful.

The radome was also tested in flight to ensure that it did not cause additional drag that would jeopardize the stability of the aircraft, and had enough authority to start and stop rotation while in flight. These tests also proved successful, as there was no noticeable difference in the controllability, stability, or performance of the aircraft.

8.1.4 Power System Testing

The power system was thoroughly static tested to ensure that its performance coincided closely with that predicted by theory. The tail hook was used to secure the aircraft to a spring-loaded force scale, which allowed for monitoring of the aircraft thrust as the motor powered up and down. Across static motor testing, results were very consistent with expected performance, with the power and thrust of the system closely matching or even exceeding conservative estimates.

During static and flight tests, the motor was observed to heat up very rapidly when under heavy load. This does not pose a large problem, as the motor is only near maximum power for a limited time during takeoff before rapidly throttling down to cruising power. Nevertheless, caution was taken to always monitor power levels of the motor to avoid overheating and prevent flammable components from contacting potentially hot components.

8.2 Performance of Completed Aircraft

Short field takeoffs without the ramp were initially performed to verify the takeoff performance with varying degrees of flaps down. During testing, it was determined that the motor would be able to sustain a power of about 450W with a 10x6 propeller. This reaffirmed the theoretical power consumption of about 515W during the static testing. It was noticed that the motor was rising in temperature very quickly which is concerning given that it is still operating below the motor's power limit of 500W. After a few tests the thrust generated by the propeller exceeded the tensile strength of the foam that was used to connect the firewall to the rest of the fuselage. To remedy this problem longer screws were used to anchor the firewall deeper into the foam.

Landing gear deflects the amount that was calculated under the normal loading of the plane. The landing gear is designed so that on landing when the gear impacts with the ground, much of the force will

be transferred to the elastic bands connecting the axles, preventing damage to the landing gear. After testing it was discovered that the impact has enough force to slightly yield the aluminum frame but the overall shape was still maintained by the elastic band.

9. Bibliography

[1] Anderson, John D. *Fundamentals of Aerodynamics*, 5th Edition, McGraw-Hill, Boston, 2011. Print.

[2] Cazes, Cristophe. "Electric Folding Wing for Car Composite Corsair." Online video clip. Youtube. Google, 11 April 2015. Web. October 2018. https://www.youtube.com/watch?v=9Y0Mfv7uPjo.

[3] Staples, Gabriel. “Propeller Static & Dynamic Thrust Calculation - Part 2 of 2 - How Did I Come Up With This Equation?” *ElectricRCAircraftGuy.com--RC, Arduino, Programming, & Electronics*, 1 Jan. 1970, www.electricrcaircraftguy.com/2014/04/propeller-static-dynamic-thrust-equation-background.html.

[4] "UIUC Airfoil Data Site." *UIUC Applied Aerodynamics Group*. N.p., n.d. Web. 21 Nov. 2018. http://m-selig.ae.illinois.edu/ads/coord_database.html.